Research Square

Preprints are preliminary reports that have not undergone peer review.
They should not be considered conclusive, used to inform clinical practice,
or referenced by the media as validated information.

Multidimensional analysis of the effects of drought stress on chlorophyll synthesis in Lonicera japonica leaves

Haizhen Wang
Lyuliang University
Boxiang Zhang
Lyuliang University
Caiping Feng
Lyuliang University
Xia Zhang
20211020@llu.edu.cn

Lyuliang University

Research Article

Keywords: Lonicera japonica, Drought stress, Chlorophyll synthesis, Metabolome, Transcriptome

Posted Date: September 3rd, 2024

DOI: https://doi.org/10.21203/rs.3.rs-4875887/v1

License: This work is licensed under a Creative Commons Attribution 4.0 International License.
Read Full License

Additional Declarations: No competing interests reported.

Multidimensional analysis of the effects of drought stress on chlorophyll synthesis in *Lonicera japonica* leaves

Haizhen Wang, Boxiang Zhang, Caiping Feng*, Xia Zhang*

Department of Biological and Food Engineering, Lyuliang University, Lvliang 033300, China

***Corresponding author**

E-mail address: Caiping Feng 627752817@qq.com; Xia Zhang 20211020@llu.edu.cn

Abstract

Background *Lonicera japonica* is an important medicinal plant, and its drought resistance is often related to the yield and the economic income of farmers. The drought resistance of plants is closely related to the mechanism of chlorophyll synthesis and decomposition. At present, many scientific reports have focused on the effects of drought stress on photosynthesis and chlorophyll content of *L. japonica*, but have not studied the chlorophyll anabolism of *L. japonica* from the perspective of molecular mechanism and metabolic level.

Results To analyze the response mechanism of chlorophyll synthesis in honeysuckle (*Lonicera japonica*) plants under drought stress and to screen for the key regulatory genes and precursor metabolites associated with chlorophyll synthesis, a control group (CK) and three experimental

groups, which were subjected to light stress (L), moderate stress (M), or severe stress (S), were established in this study. The mechanism of chlorophyll synthesis in *L. japonica* leaves under drought stress was comprehensively analyzed at the physiological, biochemical, transcriptional, and metabolic levels. Physiological and biochemical studies revealed that with increasing drought stress, the total chlorophyll content (C_t) of *L. japonica* leaves tended to initially exhibit a slight increase and then a sharp decrease, and the content of most chlorophyll synthesis-related enzymes decreased. A total of 37,735 differential genes (DEGs) were identified by transcriptome analysis, 16 of which were related to chlorophyll synthesis. Metabolomic analysis revealed a total of 2,132 differentially abundant metabolites, 4 of which were precursors of differentially accumulated substances in the chlorophyll synthesis pathway.

Conclusions The multidimensional analysis results show that the metabolite Mg-protoporphyrin IX monomethyl ester and the closely related gene *HEMA1* may be key precursors of chlorophyll synthesis and key regulators of chlorophyll synthesis in *L. japonica* during drought stress. However, the mechanism of the influence of *HEMA1* and Mg-protoporphyrin IX monomethyl ester on chlorophyll synthesis under drought stress has yet to be explored. This study is highly important for furthering the understanding of drought resistance mechanisms in medicinal plants and for molecular breeding to produce new varieties of honeysuckle with strong drought tolerance.

Keywords: *Lonicera japonica,* Drought stress, Chlorophyll synthesis, Metabolome, Transcriptome

Introduction

Lonicera japonica, a member of the honeysuckle family, is known for the natural antimicrobial effects of its dry buds and initial flowers and is produced mainly in Pingyi in Shandong Province, Fengqiu in Henan Province, and Julu in Hebei Province, China. *L. japonica* can clear heat and has detoxification properties; thus, it is commonly used as a bulk Chinese herbal medicine [1]. For the past few years, with the spread of various epidemics, the gap between the supply and demand of *L. japonica* has become more prominent. Thus, *L. japonica* has become the leading species in the Chinese herbal medicine market and has high economic value and very broad market prospects. However, due to the limitations of the arid climate in northern China, the *L. japonica* yield is low, and farmers are reluctant to plant *L. japonica*, seriously hindering the development of the *L. japonica* industry in China. Therefore, it is important to study the drought resistance mechanism of *L. japonica* and cultivate *L. japonica* varieties with strong drought tolerance.

Chlorophyll, including chlorophyll a and b, is an important pigment for plants that participates in photosynthesis. Chlorophyll synthesis is very complex and involves 15 enzymatic reaction stages in which the enzymes involved are encoded by more than 20 related genes [2-3] (Fig. 1). The first stage of chlorophyll synthesis is from L-glutamyl-tRNA to protoporphyrin IX (proto IX). First, L-glutamyl-tRNA is reduced to L-glutamic acid 1-semialdehyde by glutamyl-tRNA reductase (Glu-tRNAs), and complete tRNA is released. Then, L-glutamic acid 1-semialdehyde is catalyzed by glutamate 1-semialdehyde aminomutase (GSA) to form δ-aminolevulinic acid

(ALA). The genes encoding the two enzymes involved are *HEMA, HEML*, and *GSA*. ALA is catalyzed by 5-aminolevulinate dehydratase (ALAD) to form porphobilinogen (PBG), which involves the gene *HEMB.* Porphobilinogen deaminase (PBGD), encoded by *HEMC,* can catalyze the transformation of PBG to linear hydroxymethylbilane (Hmb). *HEMD*-encoded urogen III synthase catalyzes the intramolecular rearrangement of linear Hmb to form the common precursor of the tetrapyrrole compound uroporphyrinogen III (urogen III). Coproporphyrinogen III (coprogen III) is synthesized after the decarboxylation of 4 acetic acid groups in the side chain of Urogen III. The enzyme that plays a catalytic role in the reaction is uroporphyrinogen III decarboxylase (UROD), whose coding gene is *HEME.* Coprogen III forms protoporphyrin IX (proto IX) through a two-step oxidation reaction. The enzymes involved in the two-step oxidation reaction are coproporphyrinogen III oxidative decarboxylase (CPOX) and protoporphyrinogen oxidase (PPO), and the encoded genes are *HEMF* and *HEMG*, respectively. The second stage is from proto-IX to chlorophyll. The chlorophyll molecule is mainly a porphyrin ring containing Mg^{2+}; thus, in this step, Mg^{2+} is first added to the porphyrin ring of proto IX through the catalysis of Mg-chelatase (MgCH) to generate Mg-protoporphyrin IX (Mg-proto IX). MgCH is expressed and regulated by *CHLD, CHLH*, and *CHLI.* Mg-proto IX is methylated to MG-protoporphyrin IX methyl ester (Mg-PME) by the catalysis of MG-protoporphyrin IX methyltransferase (CHIM), the encoding gene of which is *CHIM*. Mg-PME is catalyzed by the Mg-protoporphyrinogen IX monomethylester cyclase (Mg-ProtoIX Cyclase) to form divinyl protochlorophyllide, the regulatory gene of which is *CRD1*. Under the

catalytic action of divinyl reductase (DVR), the C-8 position of divinyl protochlorophyllide is converted to an ethyl group to form protochlorophyllide (pchlide). This reductase is a key enzyme for the synthesis of normal monovinyl chlorophyll (MV-Chl) in plants, and its regulatory gene is *DVR*. Pchlide needs protochlorophyllide oxidoreductase (POR) to reduce to chlorophyllide (chlide) under light conditions. The three genes that regulate this reaction are *PORA*, *PORB*, and *PORC*. Chlide b is formed by the chlide c-7 methyl group catalyzed by chlorophyllide a oxygenase (CAO), whose coding gene is *CAO* (*CHL*). Chlide b is subsequently catalyzed by the chlorophyll synthase (CHLG) gene, which is encoded by *CHLG,* to chlorophyll b (Chl b). In addition, chlide a can also be directly catalyzed by CHLG to form chlorophyll a (Chl a). Several researchers have identified genes involved in chlorophyll synthesis in *Arabidopsis* [2], rice [4] , barley [5], tobacco [6], and maize [7]. The study of the expression of these genes is highly important for exploring the molecular regulatory mechanism of chlorophyll synthesis in plants.

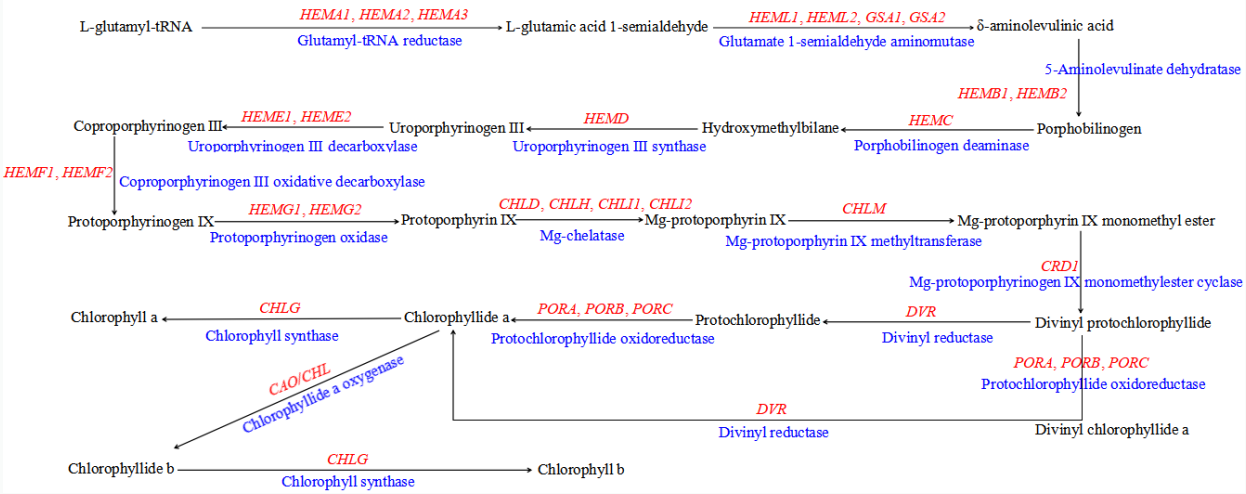


Fig. 1 Chlorophyll biosynthesis pathway in angiosperms. Red represents chlorophyll synthesis

regulatory genes, blue represents chlorophyll synthesis-related enzymes, and black represents intermediate products related to chlorophyll synthesis. The chlorophyll synthesis-related enzymes in the figure are consistent with those in Table S1

Since plants are sessile and therefore limited to existing only in their original environment, their growth and development are easily affected by abiotic factors, such as salinity stress, drought stress and heavy metal pollution [8]. Drought, as one of the major abiotic stress factors, affects the normal growth and development of plants and inhibits increases in crop yield [9]. In the initial stage of drought, the water potential of plant leaves decreases, and the stomata close, which reduces CO_2 intake and photosynthetic efficiency; however, the photosynthetic system is not damaged [10]. However, with the intensification of drought stress, the photosynthetic system and function of plant leaves are damaged, and the lamellar structure of leaves is especially adversely affected, with chlorophyll synthesis being blocked and disrupted, resulting in reduced chlorophyll content, changes in photosynthetic physical properties, and the yellowing and wilting of plant leaves [11]. According to studies on the responses of wheat [12] and maize [9] to drought stress, drought stress can reduce chlorophyll content, change fluorescence parameters, and inhibit photosynthetic electron transfer, thus reducing the photosynthetic rate. Therefore, the chlorophyll content directly affects leaf photosynthesis and is an important index for measuring the drought resistance of plants. *L. japonica* plants exhibit drought tolerance, and exhibit a very strong ability to adapt to soil and climate. To date, many scientific reports have focused on the

effects of drought stress on photosynthesis and chlorophyll content in *L. japonica* [13-16]; however, these studies focused on superficial assessments of chlorophyll physiology and biochemistry and did not include in-depth studies of *L. japonica* chlorophyll anabolism from the perspective of molecular mechanisms and metabolic levels. With the development of transcriptome sequencing and chromatography–mass spectrometry, it has become a trend to analyze the internal mechanism of plant growth and development by using integrated omics. Plant metabolic and physiological mechanisms can be systematically studied from macro- and microperspectives by combining plant external trait observations and physiological and biochemical analyses. Through transcriptomic and metabolomic analyses, Yang et al [17] revealed the molecular regulatory mechanism of secondary metabolites during the development of honeysuckle petals. Similarly, Xue et al [18] and Xia et al. [19] clarified the *L. japonica* pigmentation mechanism at different developmental stages via transcriptomics and targeted metabolomics. This paper describes the response mechanism of chlorophyll synthesis in *L. japonica* under drought stress at the physiological, biochemical, transcription, and metabolic levels and identifies key regulatory genes and precursor metabolites that affect chlorophyll synthesis. It is highly important to cultivate new varieties of *L. japonica* with strong drought tolerance via molecular biology.

Material and methods

Test plants and drought-stressed environments

The *L. japonica* (2-year-old) plants used in the experiment were obtained from Jiujianpeng Ecological Agriculture Development Co., Ltd., Pingyi County, Shandong Province, and planted in Liulin county, Luliang city, Shanxi Province. The average plant height was 52.6 cm, and the average ground diameter was 2.3 cm. This variety was identified as 'Beihua No. 1' by Li Weidong, a professor at the Beijing University of Chinese Medicine and chairperson of the China Economic Forest Association Honeysuckle Professional Committee.

The drought stress test was carried out by first watering the soil and then stopping the watering to artificially control the soil moisture [20]. On June 12, 2023, 100 biennial 'Beihua No. 1' plants from the standardized planting base of the introduced *Lonicera japonica* plant in Luliang Mountain were planted in pots (diameter: 40 cm) and loaded with nutrient soil (pH=7.3). One plant in each pot was put into the greenhouse for normal maintenance and management. After the adaptation period, 30 uniformly sized plants with robust growth were randomly selected for maintenance in the greenhouse for the drought stress test. To prevent high-temperature stress in the greenhouse, the greenhouse was cooled by spraying the roof with cold water and ventilation. The average temperatures and relative humidity during the day and at night were 28/20°C and 60/65%, respectively. One day before the test, water was poured so that the substrate was in a state of saturated water, and no additional water was applied until the end of the test. The first day after watering was the baseline drought stress treatment (control group, CK), the third day was the light stress group (L), the sixth day was the moderate stress group (M), and the 15th day was the severe stress group (S). The relative water content (%) of the soil in the test pot was

157 measured by a soil moisture detector (YUNTANG, Weifang, China) at 5:00 PM every day. The
158 relative water content of the soil in the CK treatment was 85%-90%, that in the L treatment was
159 70%-75%, that in the M treatment was 40%-45%, and that in the severe stress (S) treatment was
160 20%-25% [14]. At each stress stage, the top *L. japonica* leaves were taken from 8:30 am to 9:30
161 am for morphological observation and then stored at -80°C for further experiments.
162
163 **Leaf morphology observation and color index detection**
164 The morphological characteristics of the *L. japonica* leaves were observed and recorded under
165 each drought stress environment, and the color indices of the leaves were determined via a
166 colorimeter (FRU, WF30, Shenzhen, China). Six randomly sampled leaves, as six biological
167 replicates, were laid flat on the test port of the colorimeter for color index determination. The
168 standard samples for color difference analysis were collected from the leaves of the control
169 group plants. The color characteristics of each test leaf from the drought stress group were
170 compared with those of the standard sample from the control group. The test color characteristics
171 were the red–green value (*a*), yellow–blue value (*b*), brightness value (*L*) and total color
172 difference value (ΔE). The measuring conditions of the colorimeter were as follows: light source
173 D65, light mode SCI, measuring aperture of 8 mm, and standard observation angle of 10°.
174 **Detection of leaf physiological and biochemical indices**
175 In the control group (CK) and each stress group (L, M, and L), a total of 30 leaves from the
176 upper part of each test plant were mixed, and the middle veins of the leaves were removed and

177 cut with scissors into fragments approximately 5 mm in diameter. The leaves were then evenly
178 divided into 3 parts as 3 replicates.

179 **Chlorophyll content detection**

180 According to the instructions for the plant chlorophyll content kit (Keming Biology, Suzhou
181 Keming Biotechnology Co., Ltd., Suzhou, China), the chlorophyll of *L. japonica* leaves was
182 extracted with acetone. The specific method is as follows: 0.1 g of leaf fragments from each
183 replicate sample was transferred to a mortar. Then, 1 mL of distilled water and 50 mg of reagent
184 1 were added to the mortar, and the samples were fully ground into a homogenate in a dark
185 environment before transferring the samples to a 10 mL glass test tube. The chlorophyll extract
186 was prepared according to a ratio (1:4) of distilled water:acetone, and the mortar was rinsed with
187 the extract. All the rinsing liquid was put into a glass test tube, after which the mixture was filled
188 with the extract to 10 mL. The glass tube was placed on tin foil and soaked for 3 h in the dark.
189 When the leaf residue at the bottom of the glass tube was completely white, the chlorophyll was
190 considered fully extracted; if the residue was not completely white, the extraction continued. One
191 milliliter of the chlorophyll-containing extract was added to a 1 mL glass cuvette, after which the
192 extract was used for zero correction. The absorbance was measured by a spectrophotometer
193 (MRCY, UV1500-PC, Shanghai, China) at 663 nm and 645 nm, and the total chlorophyll content
194 (C_t), chlorophyll a content (C_a), and chlorophyll b content (C_b) were calculated according to the
195 following formulas:

196 C_t (mg/g) = $(20.21\times A_{645}+8.02\times A_{663})\times V\times D/(m\times 1000)$

C_a (mg/g) = (12.7×A_{663}-2.69×A_{645})×V×D/(m×1000)

C_b (mg/g) = (22.9×A_{645}-4.68×A_{663})×V×D/(m×1000)

V: extraction liquid volume, 10 mL; D: dilution ratio, 10; m: sample mass, 0.1 g

Determination of related enzymes in the chlorophyll synthesis pathway

Enzyme-linked immunosorbent assays (ELISAs) were used to determine the concentrations of 15 enzymes (Table S1) related to chlorophyll synthesis in *L. japonica* according to the kit instructions (Ceaibo Biological, Shanghai Ceaibo Biological Technology Co., Ltd., Shanghai, China). The specific experimental procedure was as follows: 1) Sample treatment: In a mortar, 0.1 g of leaf tissue was combined with PBS buffer (1 mL, pH=7.4) and fully ground into a homogenate. Then, the homogenates were transferred to 2 mL centrifuge tubes for centrifugation at 4°C for 20 min (3000 r/min), after which the supernatant was collected for enzyme activity detection. 2) Sample addition: In a 96-well plate, 50 μL of standard solutions of different concentrations (Table S1) were added to the standard wells of a 96-well plate; 40 μL of sample diluent and 10 μL of sample were added to the sample wells. Three technical repetitions were performed for each sample. 3) For the addition of standard enzyme reagents, 100 μl of standard enzyme reagent was added to the standard and sample wells. 4) Incubation: After the 96-well plate was sealed with sealing plate film, it was incubated in a constant temperature incubator at 37°C for 60 min. 5) Wash liquid preparation: The concentrated washing solution was diluted 20 times with distilled water for subsequent use. 6) The label plate was washed, the sealing plate film was carefully removed, the liquid was discarded, the plate was shaken dry, each well was

filled with washing liquid, the plate was left for 30 seconds, and the plate was discarded; this process was repeated 5 times, and the plate was finally patted dry. 7) Chromogenic reaction: 50 µl of color developing agents A and B were added to each well, the mixture was gently shaken, and the mixture was reacted at 37°C without light for 15 min. 8) Termination reaction: The reaction was terminated by adding 50 µl of termination liquid to each well, at which point the liquid in the well turned yellow. 9): Absorbance: The absorbance (OD) of each well was measured at 450 nm with an enzyme and adjusted to zero with a blank well. The measurement was completed within 15 minutes after adding the termination solution.10): Standard curve generation: The standard product concentration was the abscissa, the OD value was the ordinate, the standard curve was generated in Excel, and the standard curve equation was obtained. 11): Calculation of the enzyme concentration in the samples: The OD value measured for the sample was substituted into the standard curve equation to determine the corresponding enzyme concentration.

RNAseq

RNA extraction, library construction, sequencing and data quality control

Total RNA was extracted from leaf tissue samples from the control group (CKT) and three drought stress groups (light stress group: LT, moderate stress group: MT, and severe stress group: ST) using TRIzol according to the kit instructions (Invitrogen, CA, USA). Three biological replicates were analyzed for both the drought stress and control groups. According to the methods of the NEBNext® Ultra™ RNA Library Prep Kit for Illumina® (NEB, Beijing, China),

1 μg of qualified RNA was used to construct a cDNA library. The sequencing was subsequently completed on a MGI-SEQ 2000 sequencing platform provided by Frasergen Bioinformatics Co., Ltd. (Wuhan, China). The raw image data files obtained by high-throughput sequencing were converted into original sequencing sequences by base recognition analysis, namely, the raw reads. Clean reads were obtained by filtering the raw reads using SOAPnuke software (v2.1.0) [21].

Clean read mapping to reference genomes and gene expression level analysis

To identify the genes with transcribed clean reads, the clean reads to the reference genome of *L. japonica* (accession no. GWHAAZE00000000) [22] were matched using HISAT2 software [23]. Moreover, using RSEM [24], the Bowtie2 [25] comparison results were used for statistical analysis, the number of reads relative to each transcript of each sample was obtained, and fragments per kilobase per million bases (FPKM) [26] conversion was performed.

Differential gene expression analysis

DEGseq2 [27] was used to analyze the gene expression differences between samples. At the same time, differentially expressed genes (DEGs) were screened according to the following criteria: FDR< 0.05 and $|\log_2\text{-fold change}|>1$. Gene Ontology (GO) and Kyoto Encyclopedia of Genes and Genomes (KEGG) enrichment analyses were performed using GOseq [28] and KOBAS [29], respectively.

RT–qPCR of DEGs

To verify the authenticity of the RNA-seq data, 16 DEGs (with three biological replicates for

each DEG) related to chlorophyll synthesis in *L. japonica* were selected for real-time quantitative PCR (RT–qPCR) and primers were designed with Primer Premier 5.0 software (Table S2). According to the instructions of the THUNDERBIRD SYBR qPCR Mix Kit (TOYOBO, Japan), a LightCycler® 480, II/96 high-throughput real-time quantitative fluorescent PCR instrument (Roche, Rotkreuz, Switzerland) was used to perform real-time fluorescent quantitative PCR amplification according to the following procedure: 94°C for 60 s of preincubation and 40 cycles of 94°C for 5 s, 60°C for 15 s, and 72°C for 10 s [18]. The *L. japonica actin* gene was used as an internal reference gene [30], and the relative expression levels of each gene were calculated via the $2^{-\Delta\Delta C}$ method [31].

Metabolome analysis

Tissue treatment of Lonicera japonica leaves

Thirty leaves from the top of *L. japonica* plants were collected from the control group (CKM) and three drought stress groups (mild stress: LM, moderate stress: MM, severe stress: SM). After mixing, the plants were randomly divided into 6 groups as 6 biological replicates for metabolic analysis. Fifty milligrams of leaf tissue from each sample was added to a 2 mL centrifuge tube, and then 500 μL of cold methanol/water (70%, v/v) was added to the centrifuge tube. All of the following operations were performed on ice. The leaf tissues in the centrifuge tube were homogenized 4 times, for 30 s at 30 Hz each time, oscillated for 5 min, and rested on ice for 15 min. The mixture was centrifuged at 4°C and 12000 rpm for 10 min, after which 400 μL of the supernatant was transferred to another centrifuge tube. Then, 500 μL of ethyl acetate/methanol

(v/v, 1:3) was added to the precipitate in the first centrifuge tube, which was shaken for 5 min and left on ice for 15 min. The samples were subsequently centrifuged at 4°C and 12000 rpm for 10 min, after which 400 μL of the supernatant was removed. After two centrifugations, the supernatants were combined; after concentration, 100 μL of 70% methanol/water was added to the dry mixture, and ultrasonication was performed for 3 minutes. The mixture was subsequently centrifuged at 4°C and 12000 rpm for 3 min, after which 60 μL of the supernatant was added to the corresponding line tube for liquid chromatography–mass spectrometry (LC–MS) analysis.

Conditions for HPLC

Extracts of all the samples were analyzed via an LC–MS system. The chromatographic conditions for the LC20 ultrahigh-performance liquid chromatograph (Shimadzu, Chengdu, China) were as follows: a Waters T3 C18 chromatographic column (1.8 μm, 2.1×100 mm); flow rate: 0.4 mL/min; column temperature: 40°C; injection volume: 2 μL; and mobile phases A and B: water (0.1% formic acid) and acetonitrile (0.1% formic acid), respectively. The gradient program used was as follows: 95:5 (v/v) at 0 min, 79:21 (v/v) at 3.0 min, 50:50 (v/v) at 5.0 min, 30:70 (v/v) at 9.0 min, 5:95 (v/v) at 10.0 min, and 95:5 (v/v) at 14.0 min.

Mass spectrum conditions

Mass spectrometry analysis of the samples was performed using a Triple TOF-6600 mass spectrometer (AB Sciex, Boston, USA). The conditions for positive and negative ion mode mass spectrometry were as follows: ion spray voltages, 5500 V (+) and -4500 (-); declustering potentials, 60 V (+) and 60 V (-); ionization temperatures, 550°C (+, -); ion source, Gas1, 50 psi

297 (+, -); ion source, Gas2, 60 psi (+, -); curtain gas, 35 psi (+, -); and collision energies, 30 V (+)
298 and 30 (-).

299 **Data processing and statistical analysis**

300 ProteoWizard software was used to convert the original data obtained by LC–MS analysis.
301 Then, the XCMS program was used to extract, compare, and retain peaks. The SVR method was
302 used to correct the peak area. The peaks with deletion rates >50% were filtered in each group of
303 samples. Afterward, metabolic identification information was obtained by searching the
304 laboratory's self-built database and integrating the public database and metDNA. Finally,
305 statistical analysis was carried out with the R program. The statistical analysis included
306 univariate analysis and multivariate analysis. One-way analysis of variance (ANOVA) was used
307 to test the significance of the difference between the mean values at $P<0.05$ using SPSS software
308 (v.22.0). The Pearson coefficient was used to analyze the correlation between two variables (sig.
309 2-tailed, $P<0.05$).

310

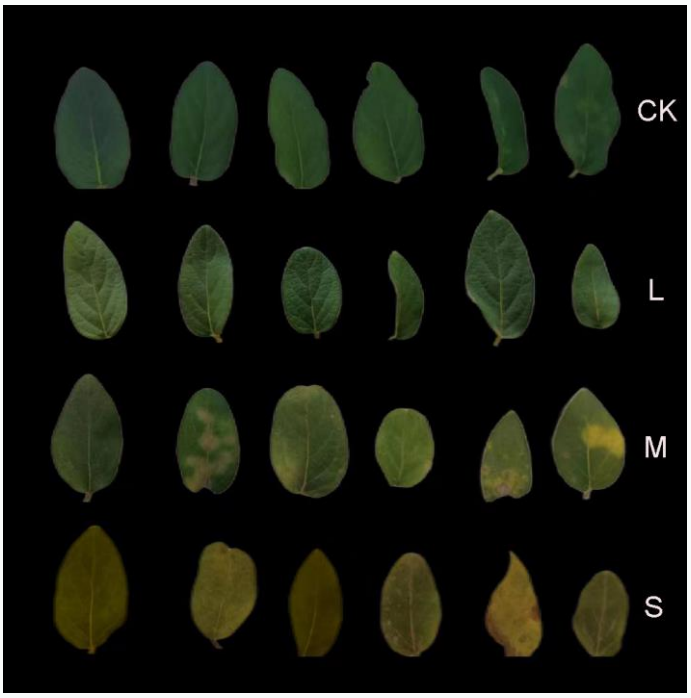
311 **Results**

312 **Observations of leaf morphology and color and determination of physiological and**
313 **biochemical indices of L. japonica plants under drought stress**

314 **Leaf morphology and color characteristics**

315 According to our tracking observations, with the worsening of drought, the *L. japonica* leaves
316 gradually turned yellow, and the leaves presented spots and curled morphology during the severe

317 stress (S) stage (Fig. 2). Similarly, the leaf color indices also showed different trends with
318 increasing drought stress. With increasing drought stress, the change in the light value (*L*) was
319 not significant ($P>0.05$), but the total color difference value (ΔE), the red/green value (*a*) and the
320 yellow/blue value (*b*) increased significantly ($P< 0.01$) (Fig. 3). In the moderate (M) and severe
321 stress groups (S), the leaf color of *L. japonica* was more red than green, and the leaf color was
322 more yellow than blue in the severe stress group (S).



323

324 **Fig. 2** Leaf morphology of *Lonicera japonica* plants in different drought stress groups

325

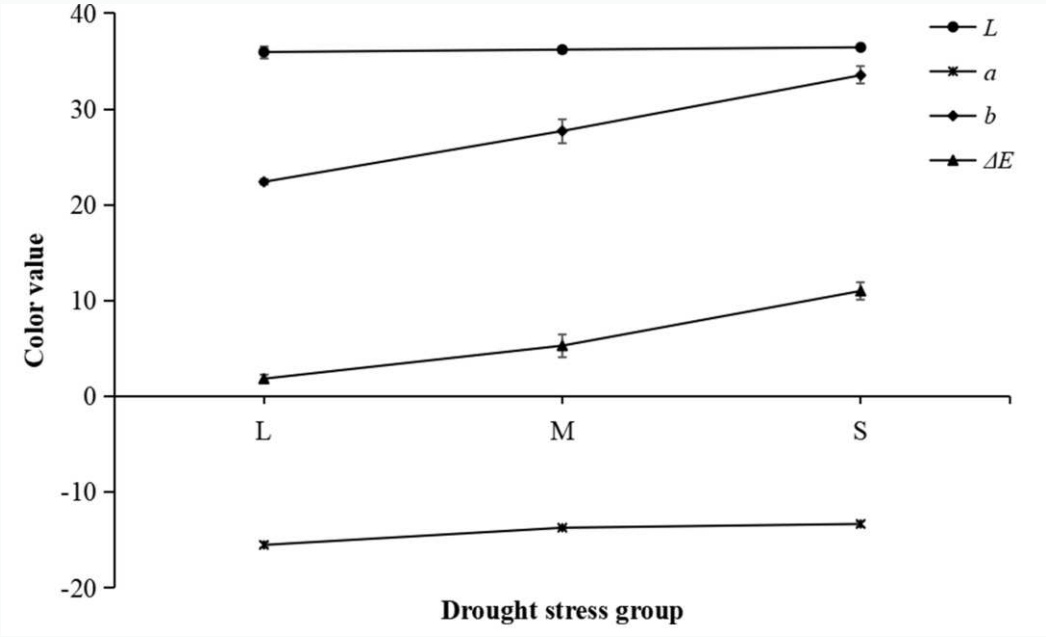
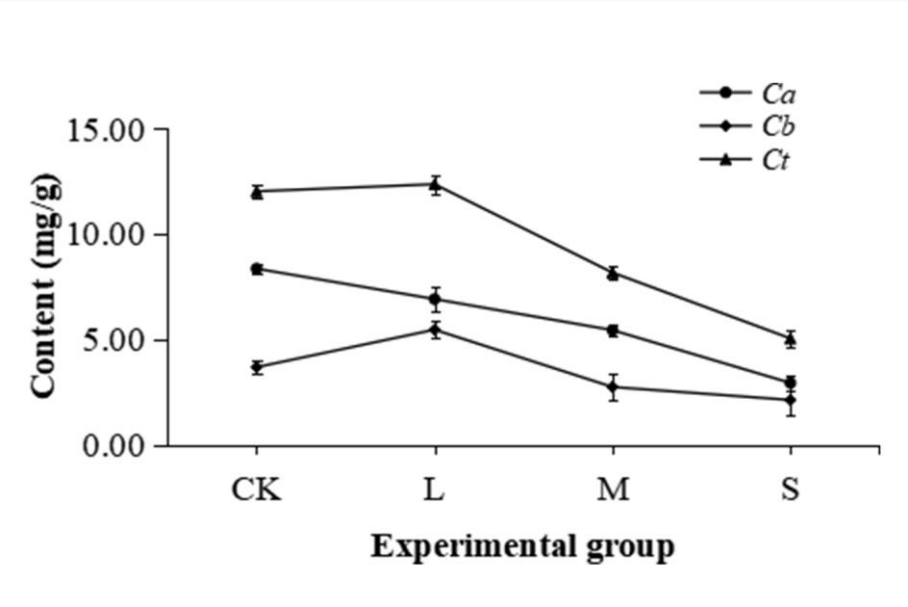


Fig. 3 Leaf color indices of *Lonicera japonica* plants in different drought stress groups

Changes in the chlorophyll content of leaves

The chlorophyll a (C_a) content was 2.92 to 8.35 mg/g, the chlorophyll b (C_b) content was 2.11 to 3.67 mg/g, and the total chlorophyll (C_t) content was 5.04 to 12.36 mg/g. The C_a content decreased gradually with increasing drought stress, but the C_b and C_t contents first increased and then decreased (Fig. 4).



334

335 **Fig. 4** Chlorophyll content of *Lonicera japonica* leaves in different drought stress groups.

336

337 **Determination of enzymes related to chlorophyll synthesis**

338 Under different drought stress conditions, the changes in 15 enzymes in the chlorophyll
339 synthesis pathway also differed among the *L. japonica* plants (Fig. 5). The concentrations of
340 GSA, Mg-proto IX cyclase, DVR, MgCH, UROD, and CHIM first increased and then decreased.
341 Glu-tRNAs and CPOX showed a continuous increasing trend. The three enzymes, PBGD, CS
342 and CAO, showed a continuous decreasing trend. ALAD and POR first decreased, then increased
343 and subsequently decreased. The UROS and PPO levels decreased first and then increased.
344 Variance analysis revealed that the concentrations of PBGD, CAO, CS, DVR, Glu-tRNAs, and
345 Mg-proto IX cyclase were significantly different among the different drought stress groups
346 (P<0.05), while those of the other 8 enzymes were not significantly different (P>0.05).

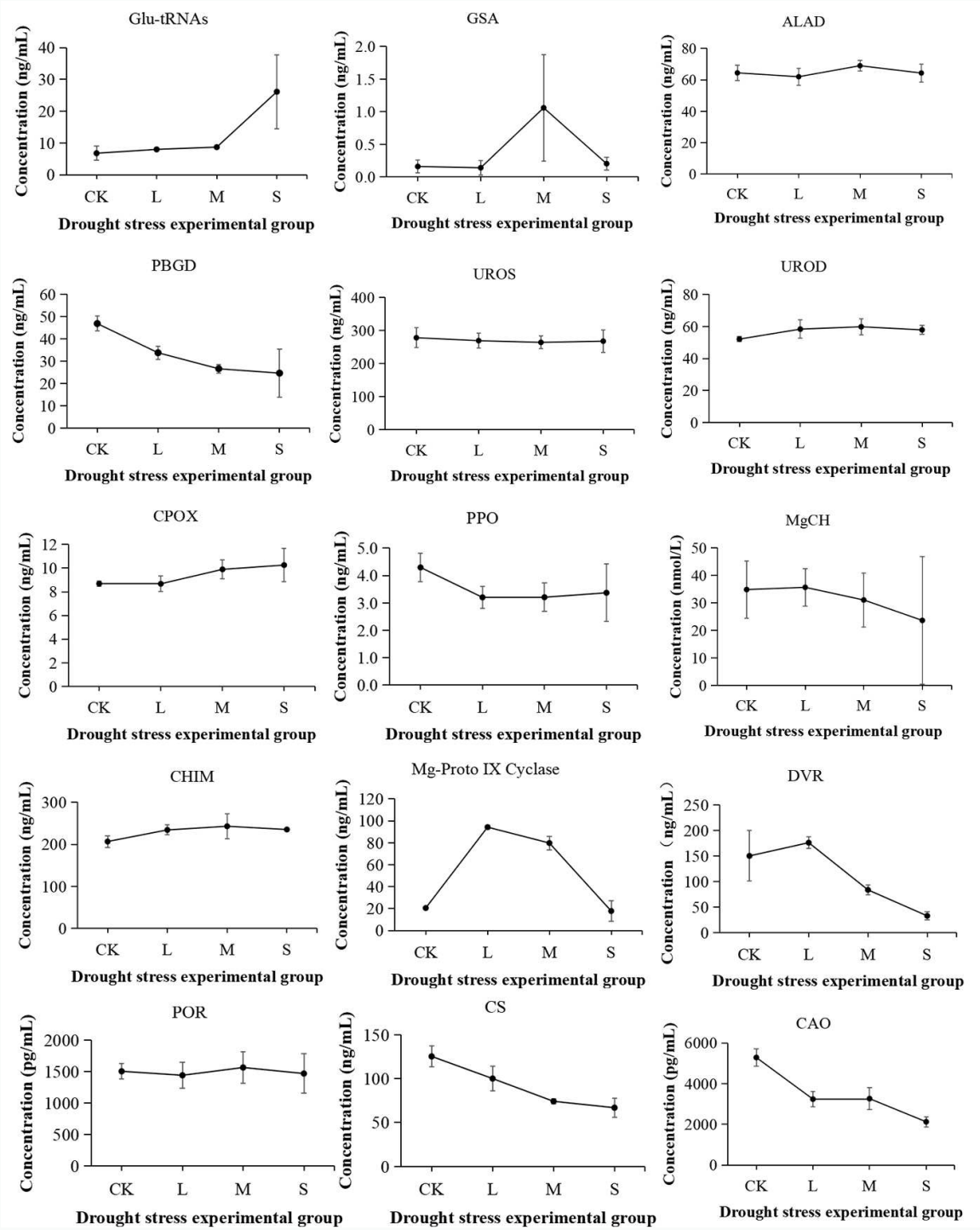


Fig. 5 Changes in the concentrations of enzymes related to chlorophyll synthesis in *L. japonica* leaves under different drought stress conditions

Transcriptome analysis under drought stress

RNA-seq and sample correlation

Transcriptomic sequencing at 4 stages (CKT, LT, MT, and ST) was conducted to determine the gene expression profile of *L. japonica* under drought stress, resulting in 12 cDNA libraries. A total of 373,915,968 clean reads with a length of 150 were obtained, ranging from 27,467,010 to 37,849,268 for each sample. The percentage of Q30 in all the samples was greater than 90.0%, indicating high-quality sequencing data. A total of 356,133,148 clean reads were compared with the reference genome of *L. japonica* to determine their gene names. A sample correlation heatmap was constructed (Fig. 6), which revealed that under the different drought stress conditions, the sample separation ability was better, the sample selection was reasonable, and the experimental results were reliable.

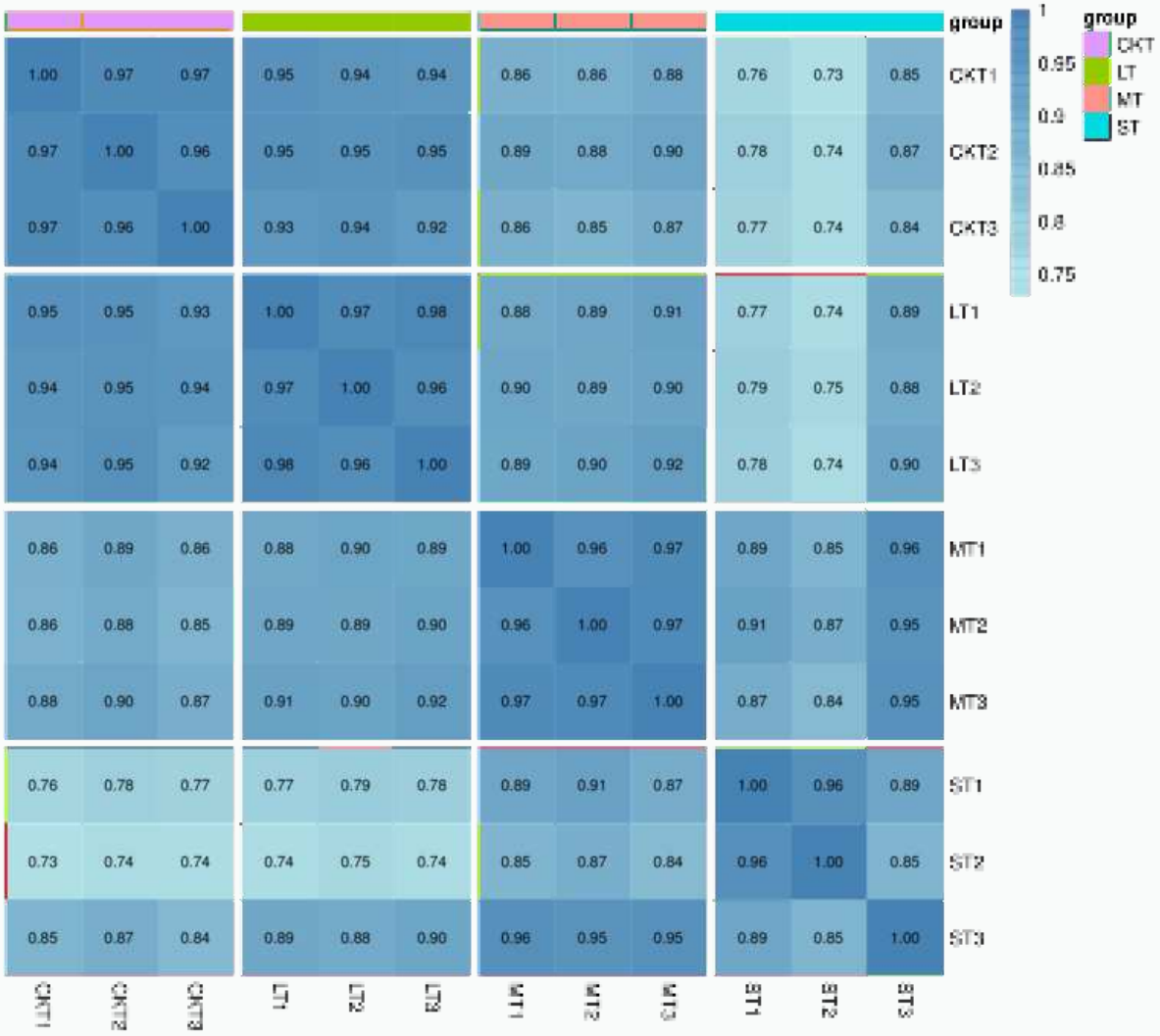


Fig. 6 Sample correlation heatmap. The data in the box are the correlation coefficients. The closer the correlation coefficient was to 1, the greater the similarity of gene expression patterns between samples.

Identification of DEGs

To study the transcriptomic differences in *L. japonica* under different drought stresses, a total of 37,735 DEGs were identified in the six pairwise comparisons (i.e., CKT vs. LT, CKT vs. MT,

CKT vs. ST, LT vs. MT, LT vs. ST, and ST vs. MT) (Supplementary Data 1). Among the six comparisons, the greatest number of DEGs was 9,983 in CKT vs. ST, among which 5,361 DEGs were upregulated and 4,622 DEGs were downregulated in ST. In contrast, the smallest number of DEGs was observed in MT vs. ST (1,655), with 1,281 and 374 up- and downregulated genes, respectively, in MT (Fig. 7). A Venn diagram of the DEGs (Fig. 8) revealed that 1,215 DEGs were shared between the stress group and the control group (CKT vs. LT, CKT vs. MT, CKT vs. ST) (Fig. 8a), and 364 DEGs were shared between the stress groups (LT vs. MT, LT vs. ST, and ST vs. MT) (Fig. 8b).

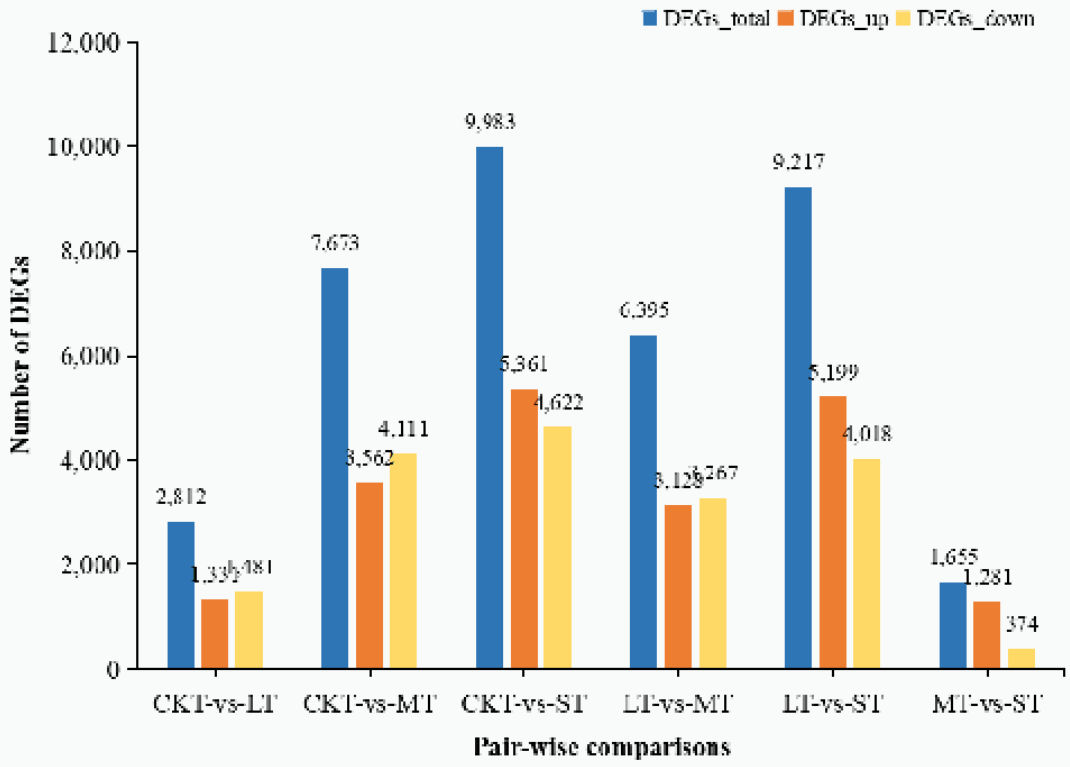


Fig. 7 Numbers of DEGs in the pairwise comparisons. CKT: control group, LT: light stress group, MT: moderate stress group, ST: severe stress group

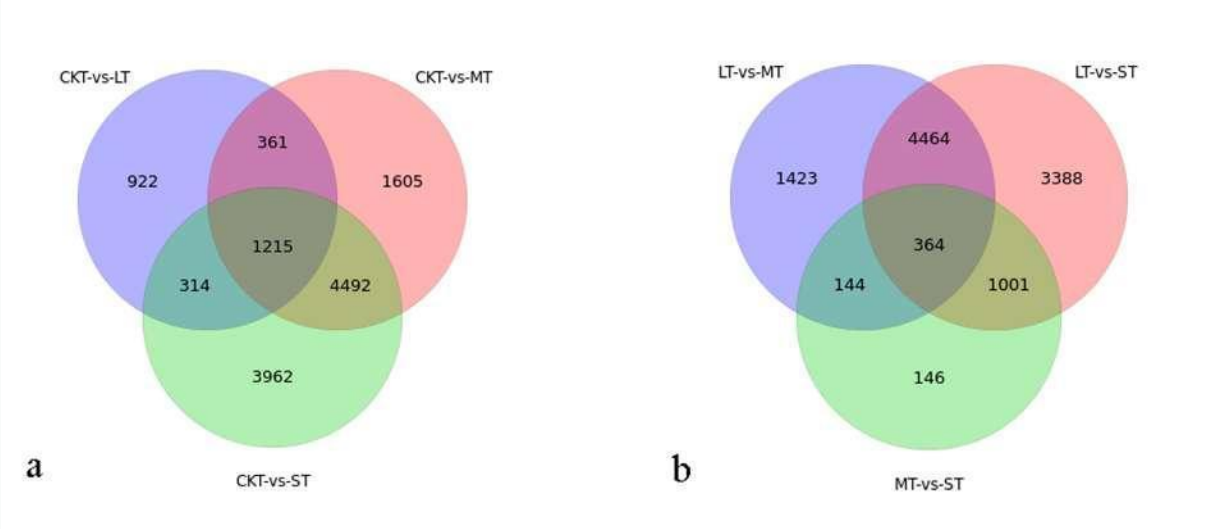


Fig. 8 Venn diagram of DEGs revealed by pairwise comparisons between the drought stress group and control group (a) and between the drought stress groups (b)

Enrichment analysis of DEGs

GO enrichment of DEGs in three pairwise comparisons (CKT vs. LT, CKT vs. MT, and CKT vs. ST) was performed (Figs. S1-S3). All DEGs were significantly enriched in three categories: molecular function (MF), biological process (BP) and cellular component (CC) (P<0.05). Among the three functions, the biological process category was associated with the most DEGs (CKT vs. LT: 834, CKT vs. MT: 856, CKT vs. ST: 863). The most enriched functional category was cellular anatomical entity (CKT vs. LT: 1,265; CKT vs. MT: 4,222; CKT vs. ST: 5,559). The enrichment bubble maps (Figs. S4-S6) of the KEGG pathways in three pairwise comparisons (CKT vs. LT, CKT vs. MT, and CKT vs. ST) revealed that all the DEGs were significantly enriched in 20 pathways (P<0.05), among which the most significant pathways were involved in

the following pathways: photosynthesis-antenna protein, circadian rhythm-plant, photosynthesis, and starch and sucrose metabolism. In addition, genes involved in the prophyrin and chlorophyll metabolism pathways associated with chlorophyll synthesis were also significantly enriched (P<0.05). To further study the signaling pathways involved in chlorophyll synthesis in *L. japonica*, the genes involved in the prophyrin and chlorophyll metabolism pathways were analyzed in three pairwise comparisons (CKT vs. LT, CKT vs. MT, and CKT vs. ST) (Figs. S7-S9). In the chlorophyll synthesis pathway, compared with those in the control group (CKT), most of the DEGs related to chlorophyll synthesis were not differentially expressed in the light stress group (LT), but most of these genes were downregulated in the moderate (MT) and severe (ST) stress groups. The nodes of these genes in the pathway were identified as EC2.5.1.61, EC4.1.1.37, EC1.3.3.3, EC1.3.3.4, and EC1.3.1.33. Moreover, several genes involved in chlorophyll synthesis were upregulated in the mild stress group (LT), but there was no difference in the expression of these genes between the moderate stress group (MT) and the severe stress group (ST). The nodes of these genes in the pathway were EC1.14.13.81, EC1.3.1.75, and EC3.1.1.14. In general, with the worsening of drought stress, the expression of genes related to the chlorophyll synthesis pathway also tended to decrease.

Analysis of DEGs in the chlorophyll synthesis pathway and RT–qPCR validation

A total of 16 chlorophyll synthesis-related genes from 11 categories were obtained from three pairwise comparisons (CKT vs. LT, CKT vs. MT, CKT vs. ST) (Table 1). Among them, three

genes (Lj9A341T44, Lju124A41T48, and Lj7A342T52) were commonly differentially expressed genes among the three comparisons. There were 5 upregulated chlorophyll synthesis-related genes, 1 downregulated chlorophyll synthesis-related gene, and 10 differentially expressed chlorophyll synthesis-related genes in the light stress group (LT) compared with those in the control group (CKT). In the moderate stress group (MT), there were 5 upregulated, 8 downregulated, and 3 differentially expressed chlorophyll synthesis-related genes. In the severe stress (ST) group, there were 4 upregulated, 6 downregulated, and 6 differentially expressed chlorophyll synthesis-related genes heatmaps (Fig. 9), and column plots (Fig. 10) of the relative expression levels showed that most of the genes related to chlorophyll synthesis were downregulated due to the exacerbation of drought stress, especially after experiencing moderate stress (MT). The variation trend of the RT–qPCR products was consistent with that of the RNA sequencing results, which verified the accuracy of the RNA-seq data (Fig. 11).

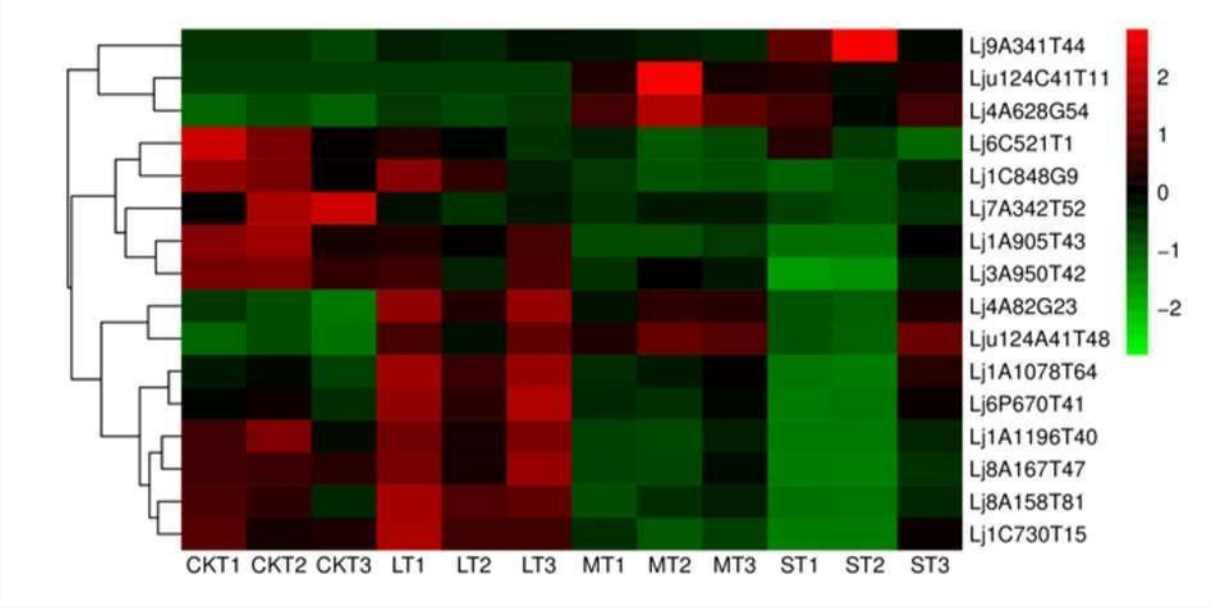


Fig. 9 Heatmap of the relative expression levels of chlorophyll synthesis-related genes. In the heatmaps, a darker color indicates greater DEG expression, and a redder color indicates lower DEG expression.

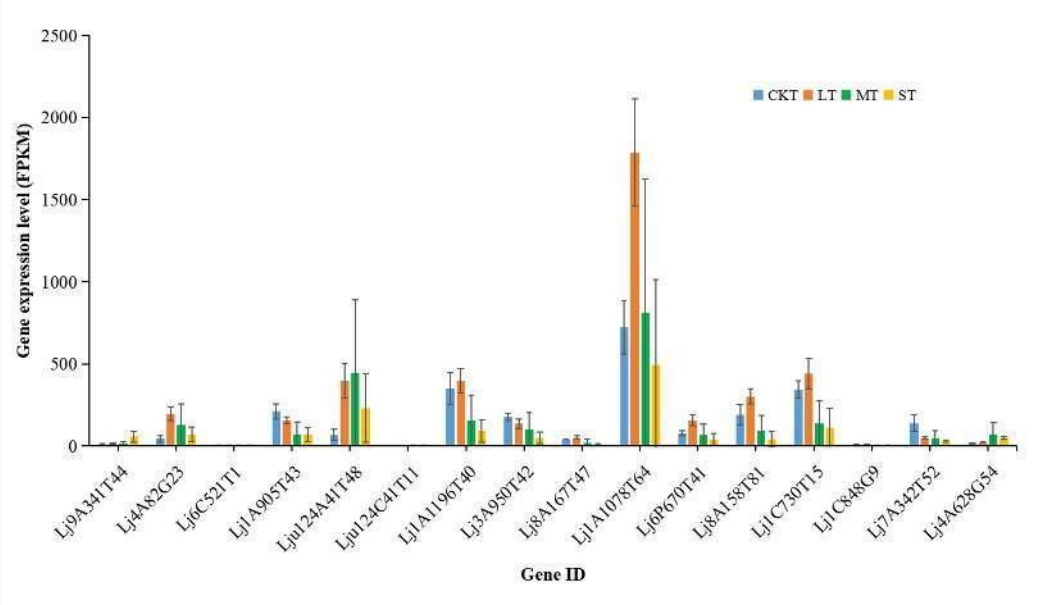


Fig. 10 FPKM values of the chlorophyll synthesis-related DEGs in three pairwise comparisons (CKT vs. LT, CKT vs. MT, and CKT vs. ST)

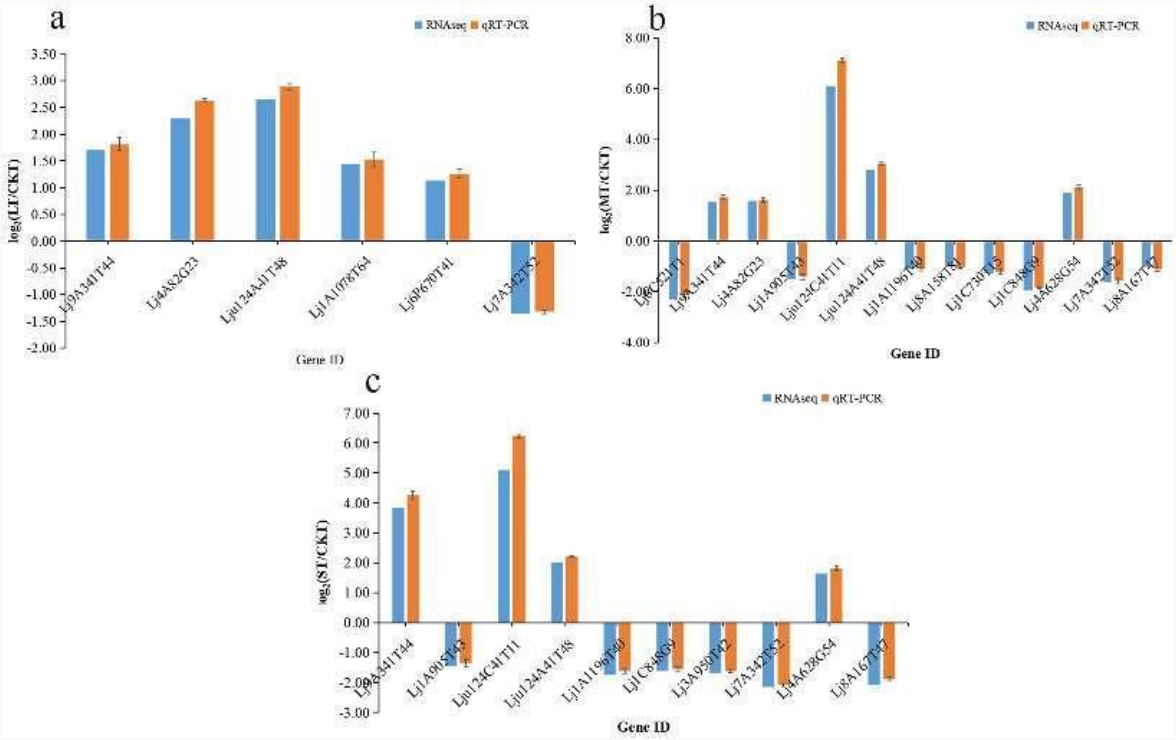


Fig. 11 RT–qPCR validation of chlorophyll synthesis-related DEGs in three pairwise comparisons: CKT vs. LT (a), CKT vs. MT (b), and CKT vs. ST (c). The yellow bar represents the RT–qPCR verification results of the DEGs, and the blue bar represents the DEGseq data resulting from the transcription of DEGs related to chlorophyll synthesis obtained from RNA-Seq. The horizontal coordinate represents the number of genes obtained from RNA-Seq. The error line of the RT–qPCR indicates the standard deviation of the average of three biological replicates. The DEGs (log2-fold change = 0) are not shown in the figure.

Table 1. Differentially expressed genes related to chlorophyll synthesis in *L. japonica*.

Gene name	GeneID	CKT vs. LT	CKT vs. MT	CKT vs. ST	Description
		log_2 fold_change[a]	log_2 fold_change[a]	log_2 fold_change[a]	
HEMA1	Lj9A341T44	1.70	1.53	3.83	glutamyl-tRNA reductase activity
	Lj4A82G23	2.29	1.57	0.00	

HEMA2	Lj6C521T1	0.00	-2.33	0.00	glutamyl-tRNA reductase activity
HEMC	Lj1A905T43	0.00	-1.51	-1.46	hydroxymethylbilane synthase activity
CHLH	Lju124A41T48	2.65	2.81	1.993	chlorophyll biosynthetic process
	Lju124C41T11	0.00	6.10	5.11	magnesium chelatase activity
CHLI	Lj1A1196T40	0.00	-1.12	-1.74	magnesium-chelatase subunit ChlI
CHLG	Lj3A950T42	0.00	0.00	-1.68	chlorophyll synthase
CHL	Lj8A167T47	0.00	-1.01	-2.09	small molecule binding
CRD1	Lj1A1078T64	1.43	0.00	0.00	magnesium-protoporphyrin IX monomethyl ester
DVR	Lj6P670T41	1.13	0.00	0.00	3,8-divinyl protochlorophyllide an 8-vinyl reductase activity
	Lj8A158T81	0.00	-1.01	0.00	protochlorophyllide reductase
POR1	Lj1C730T15	0.00	-1.29	0.00	protochlorophyllide oxidoreductase a
	Lj1C848G9	0.00	-1.93	-1.61	protochlorophyllide reductase activity
CAO	Lj7A342T52	-1.36	-1.64	-2.14	chlorophyllide a oxygenase
	Lj4A628G54	0.00	1.91	1.65	chlorophyllide a oxygenase

[a] A positive $\log_2$-fold change indicates upregulated expression of DEGs; a negative $\log_2$-fold change indicates downregulated expression of DEGs; and a $\log_2$-fold change of 0 indicates no differential expression of genes.

Metabolomic analysis in response to drought stress

Metabolite identification and data acquisition

Among the different drought stress groups (CKM, LM, MM, and SM), 4077 metabolites comprising 23 categories (Fig. 12) were identified in 24 samples using an LC–MS positive ion model (Supplementary data 2), 2,647 of which are secondary metabolites. Among the 23 categories, the maximum number of amino acids and their metabolites was 816, accounting for

20.01% of the total metabolites, followed by benzene and its derivatives at 603, accounting for 20.01% of the total metabolites. The minimum number of phenolic acid metabolites was 4, accounting for 0.1% of the total metabolites. A heatmap of metabolite accumulation (Fig. S10) showed that the metabolite accumulation pattern in the light stress (LM) group was similar to that in the control (CKM) group, but there was a difference in the metabolite accumulation pattern in the moderate stress (MM) group, and the difference observed in the severe stress (SM) group was more significant.

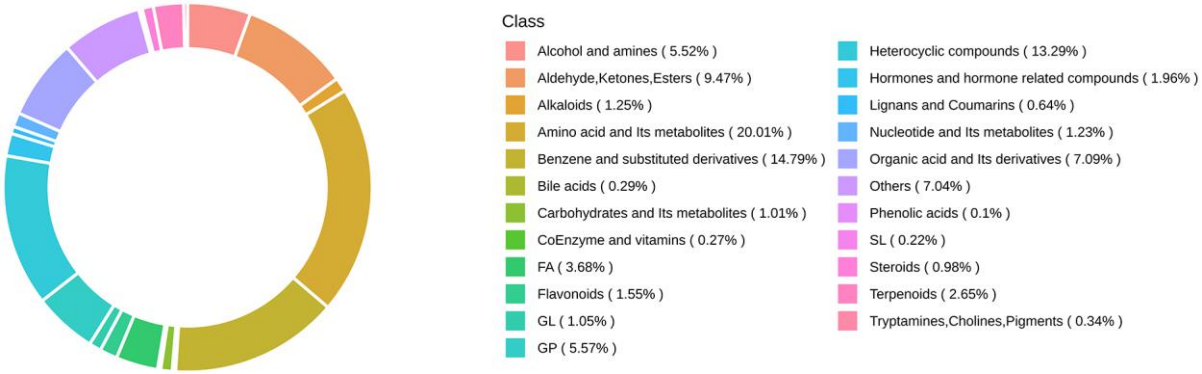


Fig. 12 Metabolite classification. A total of 4077 metabolites were identified and grouped into 23 classes

Differentially accumulated metabolite (DAM) identification and KEGG pathway analysis

Prior to the identification of differentially accumulated metabolites (DAMs), an orthogonal partial least square discriminant analysis (OPLS-OD) was first performed to determine intergroup and intragroup differences in the samples. The OPLS–OD model diagram (Fig. 13) showed that in the three pairwise comparisons (CKM vs. LM, CKM vs. MM, and CKM vs. SM),

the samples in the different drought stress groups exhibited significant separation in terms of the predicted principal components (horizontal coordinates). In the CKM vs. LM, CKM vs. MM, and CKM vs. SM comparisons, the variance explained by the predicted principal components was 21.9%, 39.5%, and 48.5%, respectively, indicating significant differences between groups for all samples.

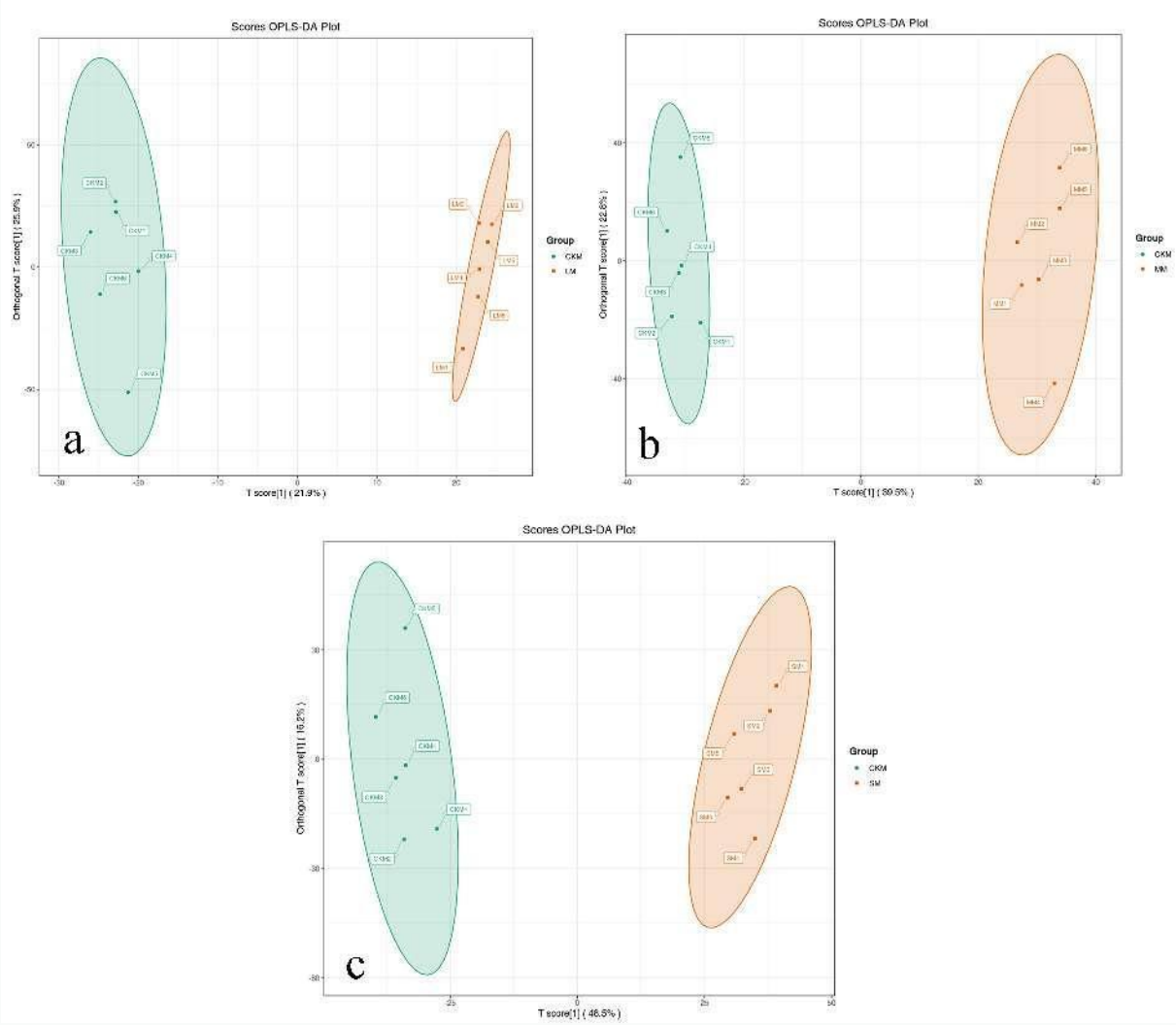


Fig. 13 OPLS-OD patterns of samples in three pairwise comparisons (CKM vs. LM, CKM vs. MM, and CKM vs. SM)

Based on the criteria of VIP>1 and P<0.05, 3,190 differentially accumulated metabolites (DAMs) were screened from three pairwise comparisons (CKM vs. LM: 633, CKM vs. MM: 1176, CKM vs. SM: 1381, LM vs. MM: 1,223, LM vs. SM: 1,397, MM vs. SM: 656) (Supplementary data 3). A Venn diagram was constructed (Fig. 14), which shows that there were 295 different metabolites between the drought stress group and the control (Fig. 14a) and 285 different metabolites between the stress groups (Fig. 14b).

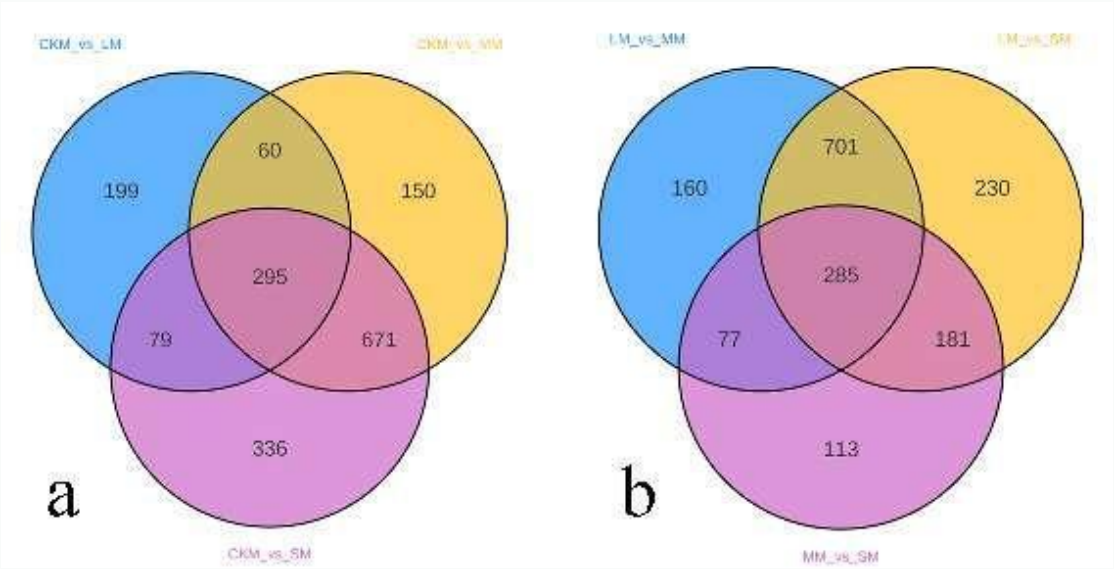


Fig. 14 Venn diagram of DAMs revealed by pairwise comparisons between the drought stress group and control group (a) and between the drought stress groups (b).

Analysis of DAMs related to chlorophyll synthesis

A total of four DAMs of chlorophyll synthesis precursors, namely, coproporphyrin III, Mg-protoporphyrin IX 13-monomethyl ester, protochlorophyllide and chlorophyllide b, were obtained from three comparison groups (CKT vs. LT, CKT vs. MT, and CKT vs. ST) (Table 2).

492 Among the four metabolites, coproporphyrin III and Mg-protoporphyrin IX 13-monomethyl
493 ester were downregulated with increasing drought stress; however, the accumulation of the
494 protochlorophyllide and chlorophyllide b metabolites was upregulated.

Table 2. Differentially accumulated metabolites involved in the chlorophyll synthesis pathway in *Lonicera japonica*.

Compound	Index	CKT vs. LT	CKT vs. MT	CKT vs. ST	Corresponding regulatory gene(s)	Corresponding catalytic enzyme(s)
		log_2 fold_change[a]	log_2 fold_change[a]	log_2 fold_change[a]		
Coproporphyrinogen III,	MW0147774	0.00	4.17	3.86	*HEME1, HEME2*	Uroporphyrinogen decarboxylase
Mg-Protoporphyrin IX 13-monomethyl ester	MW0153315	0.00	-2.37	-5.20	*CHLM*	Mg-protoporphyrin IX methyltransferase
Protochlorophyllide	MW0156149	0.00	0.00	2.45	*DVR*	Divinyl reductase
Chlorophyllide b	MW0147427	0.00	0.00	1.32	*CAO, CHLG*	Chlorophyllide a oxygenase, Chlorophyll synthase

[a] A positive log_2-fold change indicates upregulated accumulation of DAMs; a negative log_2-fold change indicates downregulated accumulation of DAMs; and a log2-fold change value of 0 indicates no differential accumulation of metabolites.

Multidimensional integration analysis

Combined transcriptome and metabolome analyses

Among the KEGG pathways of the three pairwise comparisons (CK vs. L, CK vs. M, CK vs. S), a total of 72 pathways were enriched with genes and metabolites at the same time, among which 46 pathways were mapped to CK vs. L, 67 pathways were mapped to CK vs. M, and 65 pathways were mapped to CK vs. S (Supplementary Data 4). Among these 72 pathways, the pathway related to chlorophyll synthesis in *L. japonica* leaves was porphyrin metabolism (ko00860). In the CK vs. L comparison, 13 genes and 3 metabolites were mapped to the porphyrin metabolism pathway. In the CK vs. M comparison, 25 genes and 7 metabolites were mapped to the porphyrin metabolism pathway. In the CK vs. S comparison, 21 genes and 6 metabolites were mapped to the porphyrin metabolism pathway (Table 3).

Table 3. DEGs and DAMs mapped to the porphyrin metabolism pathway in the three pairwise comparisons (CK vs. L, CK vs. M, CK vs. S).

Pairwise comparison	Metabolite ID	Metabolite number	Gene ID	Gene number
CK vs. L	MW0126592 MW0144995 MW0149544	3	Lj6C645T4, Lj7A651T30, Lj9P464T76, Lju124A41T48, Lj7A342T52, Lj6P670T41, Lj9A341T44, Lj7A567T29, Lj1A304T23, Lj8C243G1, Lj1A1078T64 Lj4A82G23, Lj6P644T21	13
CK vs. M	MW0113201 MW0147774 MW0144995 MEDP1045	7	Lj1C848G9, Lj7A342T52, Lj4A628G54, Lj5C314T1, Lj6A155G23, Lj9A341T44, Lj4A82G23, Lj1A1196T40,	25

Pairwise comparison	Metabolite ID	Metabolite number	Gene ID		Gene number
CK vs. M	MW0155689 MW0153315 MW0155687 MW0124353, MW0113201, MW0147774, MW0156149, MW0155689, MW0153315	6	Lju124C41T11, Lj8A158T81, Lj1A905T43, Lju41C50G12, Lj6C645T4, Lj1C730T15, novel.11831, Lj6A29G59, Lj6C521T1 Lj2A202G52, Lju124A41T48, Lj7A651T30, Lj8A57T61, Lj6A29G59, Lju124C41T11, Lj2A1005T32, Lj8C243G1, novel.11831, Lj1A304T23, Lj1A905T43	Lj8C243G1, Lju124A41T48, novel.1847, Lj1C213G3, Lj2A1005T32, Lj6P644T21, Lj2A202G52, Lj7A651T30, novel.21369, Lj1C848G9, Lj1C213G3, Lju41C50G12, novel.1847, Lj7A342T52, Lj9A341T44, Lj3A950T42, Lj4A628G54, Lj1A1196T40,	21

512

513 The correlation network showed the correlation between DAMs and their corresponding
514 regulatory DEGs (Fig. 15). The three metabolites associated with the porphyrin metabolism
515 pathway in CK vs. M and CK vs. S were MW0147774, MW0155689, and MW0153315; among
516 these three metabolites, MW0147774 and MW0153315 exhibited large differences in
517 accumulation (VIP>1 and P<0.05) (Table 2), indicating that drought stress may have a greater
518 impact on these two metabolites. Seven chlorophyll synthesis-related genes were significantly
519 associated with MW0147774 and MW0153315 (P<0.05), and both of these genes were
520 associated with CK vs. M and CK vs. S. The seven genes were Lj4A628G54, Lju41C50G12,

Lj2A1005T32, Lj1C213G3, Lj7A651T30, Lj9A341T44, and Lj2A202G52 (Fig. 14b and c). Among these 7 genes, only Lj9A341T44 (*HEMA1*) and Lj4A628G54 (*CAO*) were significantly differentially expressed (Table 1), indicating that drought stress may have a greater impact on the expression of these two genes. In addition, the Lj4A628G54 gene (*CAO*) was positively correlated with the corresponding metabolite MW0147774 (coproporphyrinogen III) (P<0.05). However, the Lj9A341T44 gene (*HEMA1*) was negatively correlated with the corresponding metabolite MW0153315 (Mg-protoporphyrin IX monomethyl ester) (P<0.05) (Fig. 15b and Fig. 15c). RT–qPCR also confirmed the authenticity of the expression of Lj9A341T44 and Lj9A341T44 (Fig. 11).

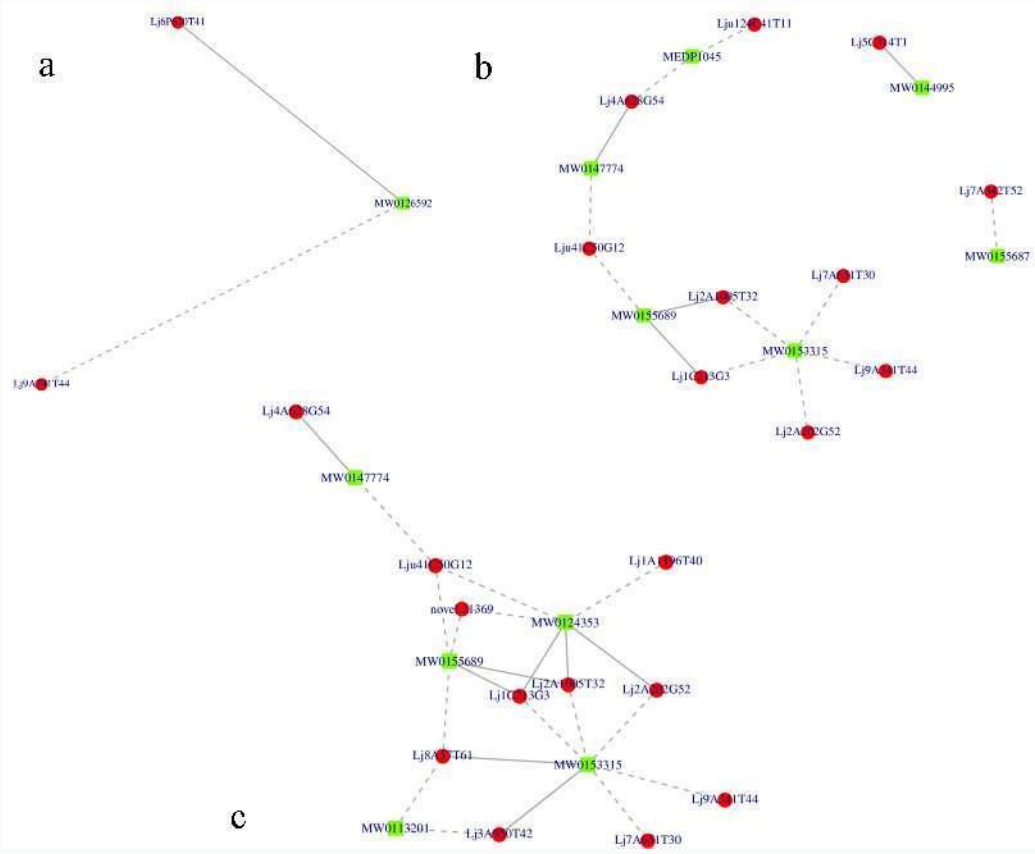


Fig. 15 Correlation network between DEGs and DAMs in the CK vs. L (a), CK vs. M (b), and

CK vs. S (c) comparisons. The Pearson correlation coefficient of DEGs and DAMs in each pathway was greater than 0.8, and the *p* value was less than 0.05. Metabolites are marked by green squares, genes by red circles, solid lines for positive correlations, and dashed lines for negative phases

Correlation analysis of enzymes related to chlorophyll synthesis and corresponding regulatory genes

The chlorophyll synthesis pathway has been reported in angiosperms (Fig. 15) [2]. To study the interactions between genes and corresponding enzymes involved in chlorophyll synthesis in *L. japonica*, Pearson correlation analysis was performed between the relative expression levels (FPKM) of DEGs related to chlorophyll synthesis (Supplementary Data 5) and the corresponding chlorophyll synthesis-related enzyme concentrations (Supplementary Data 6). As shown in Table 4, 11 of the 16 chlorophyll synthesis-related genes had a significant positive correlation with the concentration of the corresponding chlorophyll synthesis-related enzymes ($P< 0.05$), indicating that most of the genes related to chlorophyll synthesis have positive regulatory effects on chlorophyll synthesis-related enzymes during chlorophyll synthesis in *L. japonica* leaves.

Table 4. Pearson correlation analysis between the relative expression (FPKM) of DEGs and corresponding concentrations in the chlorophyll synthesis pathway.

Gene ID	Gene name	Enzyme	Pearson correlation coefficient	*P*
Lj9A341T44	*HEMA1*	Glu-tRNAs	0.986**	<0.01
Lj4A82G23			-0.375	>0.05

Gene ID	Gene name	Enzyme	Pearson correlation coefficient	*P*
Lj6C521T1	*HEMA2*		-1.590	>0.05
Lj1A905T43	*HEMC*	PBGD	0.864**	<0.01
Lju124A41T48	*CHLH*		0.580*	<0.05
Lju124C41T11		MgCH	-0.420	>0.05
Lj1A1196T40	*CHLI*		0.618*	<0.05
Lj3A950T42	*CHLG*	CS	0.924**	<0.01
Lj1A1078T64	*CRD1*	Mg-ProtoIX Cyclase	0.706**	<0.01
Lj6P670T41	*DVR*	DVR	0.731**	<0.01
Lj8A158T81			0.873**	<0.01
Lj1C730T15	*POR1*	POR	0.796**	<0.01
Lj1C848G9			0.634*	<0.05
Lj7A342T52	*CAO*	CAO	0.746**	<0.01
Lj4A628G54			-0.485	>0.05
Lj8A167T47	CHL	CAO	0.236	>0.05

One asterisk in the upper right corner of the Pearson correlation coefficient indicates a significant correlation, two asterisks indicate a highly significant correlation, and no asterisks indicate no correlation.

Correlation analysis of enzymes and precursor metabolites related to chlorophyll synthesis

Correlation analysis between the accumulation levels of four different metabolites in the chlorophyll synthesis pathway (Supplementary Data 7) and their corresponding chlorophyll synthesis-related enzyme concentrations (Supplementary Data 6) revealed that URUD and CHIM were positively correlated with the MW0147774 and MW0153315 metabolites, respectively (P<0.01). There was no significant correlation between CAO or DVR and the corresponding metabolites MW0147427 and MW0156149 (P<0.05) (Table 5).

Table 5. Pearson correlation analysis between the enzyme concentration and accumulation level of precursor metabolites related to chlorophyll synthesis.

Enzyme	Metabolite	Pearson correlation coefficient	*P*
URUD	MW0147774	0.996**	<0.01
CHIM	MW0153315	0.975**	<0.01
CAO	MW0147427	-6.300	>0.05
DVR	MW0156149	-8.920	>0.05

Two asterisks in the upper right corner of the Pearson correlation coefficient indicate a highly significant correlation, and no asterisks indicate no correlation.

Correlation analysis between precursor metabolites related to chlorophyll synthesis and chlorophyll content

The results of the correlation analysis showed (Table 6) that there was a significant positive correlation between the accumulation level of the metabolite MW0153315 and the chlorophyll content ($P<0.05$); however, three metabolites (MW0147774, MW0147427, and MW0156149) had no significant correlation with the chlorophyll content ($P>0.05$).

Table 6. Pearson correlation analysis between the accumulation levels of precursor metabolites related to chlorophyll synthesis and chlorophyll content.

Enzyme	Metabolite	Pearson correlation coefficient	*P*
Chlorophyll content	MW0147774	-0.859	>0.05
	MW0153315	0.961*	<0.05
	MW0147427	-0.871	>0.05
	MW0156149	-0.911	>0.05

Two asterisks in the upper right corner of the Pearson correlation coefficient indicate a highly significant correlation, and no asterisks indicate no correlation.

Discussion

It is highly important to explore the response mechanism of plants to environmental stress for

582 the formulation of crop variety improvement strategies. To this end, the effects of drought stress
583 (light, moderate, and severe) on the physiological, biochemical, molecular and metabolic
584 mechanisms of *L. japonica* were examined. Drought stress can hinder chlorophyll synthesis,
585 accelerate chlorophyll degradation, and ultimately lead to a decrease in plant photosynthetic
586 efficiency, affecting plant growth and development. At present, there are many studies on the
587 effects of drought stress on plant chlorophyll degradation, but few researchers have focused on
588 the effects of drought on chlorophyll synthesis. In particular, the molecular and metabolic effects
589 of drought stress on chlorophyll synthesis in *L. japonica* have not been reported thus far.
590 Therefore, this study was focused on analyzing the changes in genes and metabolites related to
591 chlorophyll synthesis in *L. japonica* under drought stress, aiming to identify the key genes and
592 precursor metabolites related to chlorophyll synthesis under drought stress and provide a
593 scientific reference for the breeding of drought-tolerant varieties of *L. japonica*.
594
595 **Effects of drought stress on the leaf morphology, color and physiological and biochemical**
596 **indices of chlorophyll synthesis in *L. japonica***
597 Over the course of long-term evolution, plants have developed a complete set of adaptive
598 mechanisms to resist stress, comprising many aspects such as morphology, structure, physiology,
599 and biochemistry. As the most sensitive organ on the ground for perceiving the external
600 environment, the leaf morphology and structure show good adaptive coordination with the
601 environment. For example, changes in leaf surface area and stomatal status play important roles

602 in regulating gas exchange and water diffusion between plants and the environment [32-33].
603 Long-term drought stress can lead to changes in the external morphology and internal structure
604 of plant leaves. Under drought stress, plants usually reduce transpiration by reducing the leaf
605 area index and single leaf area [33], which manifests as a preferential reduction in leaf width [34].
606 Long-term drought stress can also lead to changes in leaf thickness, palisade tissue, sponge tissue,
607 and other internal anatomical structures. A study on the drought resistance of *Medicago ruthenia*,
608 three species of apple and different varieties of peanut, showed that leaf structure parameters,
609 such as leaf thickness, sponge composition and palisade tissue, changed with increasing drought
610 intensity. The difference in variation is related to the strength of drought resistance in plants [35].
611 The experimental results reveal that with the intensification of drought, the leaves of *L. japonica*
612 showed different degrees of curling and wilting, and the leaf surface area and transpiration thus
613 decreased, which is an external manifestation of *L. japonica* resistance to drought stress. In
614 addition, with the intensification of drought stress, the lamellar structure of plant leaves becomes
615 damaged, chlorophyll synthesis is blocked, and chlorophyll decomposition occurs, resulting in a
616 reduction in chlorophyll content and a change in photosynthetic physical properties [36]. The
617 most intuitive manifestation of chlorophyll reduction in *L. japonica* was the gradual yellowing of
618 leaves as drought intensified (Fig. 1). Moreover, the characteristic color difference values
619 showed (Fig. 2) that in the moderate (M) and severe (S) stress groups, the leaf color of *L.*
620 *japonica* rice plants was more red and less green and more yellow and less blue, respectively.
621 This may be mainly due to the color change caused by the gradual increase in anthocyanins and

622 carotenoids during chlorophyll drought stress [37], and anthocyanin content [38] after
623 chlorophyll synthesis is blocked or degraded. In addition, in the present study, the total
624 chlorophyll content (C_t) of *L. japonica* decreased with increasing drought stress, but it increased
625 temporarily in the moderate stress group (L), indicating that *L. japonica* has strong drought
626 resistance. Similarly, the total chlorophyll content of wheat [12] and mung beans [36] also
627 decreased after drought stress, indicating that the chlorophyll content can be used as a drought
628 stress indicator in plants. The effects of drought stress on chlorophyll content are mainly
629 achieved through the synthesis and decomposition of chlorophyll by various biochemical
630 enzymes. Here, the changes in 15 enzymes related to chlorophyll synthesis under drought stress
631 were investigated. Among the 15 enzymes, only the concentrations of six enzymes (PBGD, CAO,
632 CS, DVR, Glu-tRNAs, and Mg-proto IX cyclase) were significantly different among the
633 different drought stress groups (P<0.05). Overall, the concentrations of PBGD, CAO, CS, DVR,
634 and Mg-proto IX cyclase generally decreased with increasing drought stress, especially when
635 severe drought (S) conditions were reached (Fig. 4), indicating that severe drought stress could
636 inhibit the production of these enzymes involved in chlorophyll synthesis and thus hinder the
637 synthesis of chlorophyll.
638
639 **Response of *L. japonica* leaf chlorophyll synthesis-related genes to drought stress**
640 To study the effects of drought stress on the expression of genes involved in chlorophyll
641 synthesis in *L. japonica*, the gene expression profiles of *L. japonica* leaves under different

642 degrees of drought (L, M, S) were analyzed. A total of 37,735 DEGs were screened. With the
643 control group (CK) as a reference, the number of DEGs increased with increasing severity of
644 drought (Fig. 6), indicating that drought stress had a greater impact on the gene expression
645 profile of *L. japonica*. Among these DEGs, 16 genes in the chlorophyll synthesis pathway
646 comprise 11 categories. With the increase in drought stress, the expression of most of these 16
647 genes decreased (Figs. 8 and 9), indicating that drought stress inhibited the expression of most
648 chlorophyll synthesis-related genes and decreased the content of most enzymes in the
649 chlorophyll synthesis pathway, ultimately hindering the synthesis of chlorophyll. Under drought
650 stress, the expression of genes encoding the three enzymes (ALAD, PBGD and POR) in *Triticum*
651 *aestivum* seedlings was downregulated. As a result, the activity of the encoded enzyme decreased,
652 and the contents of the intermediate products ALA, Mg-proto IV, and chlide decreased, thus
653 reducing the content of chlorophyll [39]. Similarly, Ma et al [40] reported that drought stress also
654 inhibited the expression of *PpGLTX*, *PpHMBS*, *PpUROD* and other genes related to chlorophyll
655 synthesis in *P. pratensis*. Pathway analysis of chlorophyll synthesis showed (the red dotted line
656 in Figs. 7-9) that most of the genes involved in chlorophyll synthesis were not differentially
657 expressed in the moderate stress group (L), but most of these genes were downregulated in the
658 moderate (M) and severe (S) stress groups, indicating that only when the relative water content
659 of the soil was below 40% and drought lasted for a certain period did the expression of genes
660 related to chlorophyll synthesis in *L. japonica* significantly change. Among the 16 genes related
661 to chlorophyll synthesis (Table 1), *HEMA* is encoded by Glu-tRNAs [2]. In the present study,

662 *HEMA1,* with a serial number of Lj9A341T44, was upregulated in association with the severity
663 of drought, and HEMA1 was significantly positively correlated with the concentration of
664 Glu-tRNA enzymes (Table 4), which may be an overexpression reaction of *L. japonica* after
665 activation by a transcription factor that binds to it. Therefore, the drought resistance of *L.*
666 *japonica* may be enhanced through the overexpression of *HEMA*. Under stress conditions,
667 stress-related transcription factors can bind to cis-acting elements, thereby regulating the
668 expression and signal transduction of related functional genes. The overexpression of these
669 transcription factors in transgenic plants can activate the simultaneous expression of many stress
670 resistance genes. For example, overexpression of the ERF transcription factor *TSRF1* in rice can
671 enhance drought resistance [41]. *HEMC* is the gene encoding PBGD. PBGD can catalyze the
672 conversion of orphobilinogen to hydroxymethylbilane [42]. In this study, the expression level
673 of *HEMC* (serial number: Lj1A905T43) generally decreased, revealing the inhibitory effect of
674 drought stress on *HEMC* expression. Chlorophyll is mainly composed of porphyrin rings
675 containing magnesium atoms and chlorophylls. Under the catalysis of MgCH, proto IX added
676 Mg^{2+} to the porphyrin ring to obtain Mg-proto IX. MgCH contains three subunits, namely, the H
677 subunit, I subunit and D subunit. The genes encoding MgCH in these three subunits are *CHLD,*
678 *CHLH* and *CHLI* [43-44]. In this study, the relative expression levels of the *CHLH* gene (serial
679 number: Lju124A41T48 and Lju124C41T11) and the *CHLI* gene (serial number: Lj1A1196T40)
680 decreased as drought progressed to severe stress (S), indicating that drought stress inhibited the
681 expression of the MgCH coding gene. *CHLG*, *CHL* and *CAO* are the three key genes involved in

682 the conversion of chlorophyllides into chlorophyll a and chlorophyll b. *CHLG*-encoded
683 chlorophyll synthase can catalyze the conversion of chlorophyllide a and chlorophyllide b to
684 chlorophyll a and chlorophyll b [45]. CAO, encoded by *CAO* or *CHL,* can achieve cyclic
685 conversion between chlorophyll a and chlorophyll b [46]. In this study, *CHLG* (serial number:
686 Lj3A950T42), *CHL* (serial number: Lj8A167T47), and *CAO* (serial number: Lj7A342T52) were
687 downregulated with increasing drought stress, indicating that drought stress inhibited the
688 expression of genes encoding enzymes related to chlorophyll a and chlorophyll b synthesis. *CRD*,
689 *DVR*, and *POR* are three key genes related to chlorophyll synthesis, from Mg-PME to hlide a.
690 *CRD* encodes the Mg-ProtoIX cyclase, *DVR* encodes DVR, and *POR* encodes PPO. In this study,
691 the expression of *CRD* (serial number: Lj1A1078T64), *DVR* (serial number: Lj6P670T41), and
692 *POR* (serial number: Lj8A158T81, Lj1C730T15 and Lj1C848G9) genes decreased with
693 increasing drought stress. The results showed that drought stress also affected the expression of
694 the Mg-ProtoIX cyclase, DVR, and PPO genes, which are involved in the synthesis of these three
695 chlorophyllide-related enzymes. In this study, the relative expression levels of three genes, *CRD*
696 (serial number: Lj1A1078T64), *DVR* (serial number: Lj6P670T41), and *POR* (Lj8A158T81,
697 Lj1C730T15 and Lj1C848G9), decreased with increasing drought stress. Taken together, these
698 results revealed that drought stress also had inhibitory effects on genes encoding chlorophyllide
699 synthesis enzymes.
700
701 **Response of *L. japonica* leaf chlorophyll synthesis-related metabolites to drought stress**

Metabolites related to plant synthesis under stress are generally induced by signal transduction systems, and different stress conditions lead to different levels of metabolite accumulation [47]. To study the effects of drought stress on metabolites related to the chlorophyll synthesis pathway, 4077 metabolites were identified by metabolome analysis in *L. japonica*. According to the heatmap of metabolite accumulation (Fig. 10), with the control group (CK) as a reference, the metabolite pattern in the light stress group (L) was similar, but the metabolite pattern differed from that in the moderate stress group (M) and the difference was more significant in the severe stress group (S), indicating that the metabolic level in *L. japonica* strongly changed with increasing drought stress. A total of 2,132 DAMs were screened from the three drought stress groups (L, M, and S). Among these DAMs, a total of four precursor DAMs in the chlorophyll synthesis pathway were identified. Among the four DAMs, the metabolites coprogen III and Mg-PME were both downregulated with increasing drought stress. However, pchlide and chlide b were both upregulated (Table 3). The decreased accumulation of coprogen III and Mg-PME may be related to their catalytic enzymes. The positive correlation between the accumulation levels of the two metabolites and their respective catalytic enzyme contents (UROD and CHIM) was highly significant ($P<0.01$, Table 5). The decreases in the accumulation of coproporphyrinogen III and Mg-PME may also be attributed to the negative feedback adjustment of the two downstream metabolites (pchlide and chlide b) caused by the increase in their accumulation with the aggravation of drought stress.

Key genes and precursor metabolites of chlorophyll synthesis under drought stress in *L. japonica*

To identify the key genes and precursor metabolites associated with chlorophyll synthesis in *L. japonica* in response to drought stress, the correlations between DEGs and DAMs involved in chlorophyll synthesis in *L. japonica* under drought stress were analyzed. The correlation network (Fig. 14) showed that two kinds of precursor metabolites related to chlorophyll synthesis, MW0147774 (coprogen III) and MW0153315 (Mg-PME), were mapped together in CK vs. M and CK vs. S and exhibited large differences in accumulation. The DEGs related to chlorophyll synthesis were Lj4A628G54 (*CAO*) and Lj9A341T44 (*HEMA1*), which were strongly associated with the two precursor metabolites. Of the two precursor metabolites, only MW0153315 had a significant positive relationship with chlorophyll content (Table 6). Therefore, the metabolite Mg-PME and its strongly related gene *HEMA1* may be key precursor metabolites and key regulatory genes involved in chlorophyll synthesis in *L. japonica* in response to drought stress. However, how drought stress impedes chlorophyll synthesis by affecting *HEMA1* and Mg-PME requires further investigation.

Conclusions

In this study, the effects of drought stress on chlorophyll synthesis in *L. japonica* were analyzed from the perspectives of physiology, biochemistry, the transcriptome, and the metabolome. With increasing drought stress, the leaves of *L. japonica* gradually turned yellow

and wilted, and the total chlorophyll content decreased gradually. Through the detection of gene expression and enzyme concentrations, it was concluded that under drought stress, the expression levels of most genes in the chlorophyll synthesis pathway decreased, and the content of chlorophyll synthesis-related enzymes decreased, which may correlate with a decrease in chlorophyll content. In addition, combined transcriptomic and metabolomic analysis suggested that the metabolite Mg-PME and its strongly related gene *HEMA1* may be key precursor metabolites for chlorophyll synthesis and key chlorophyll synthesis regulatory genes in *L. japonica* in response to drought stress. However, how drought stress impedes chlorophyll synthesis by affecting *HEMA1* and Mg-PME requires further exploration.

Abbreviations

ALA, δ-aminolevulinic acid; ALAD, 5-aminolevulinate dehydratase; ANOVA, One-way analysis of variance; BP, biological process; CAO, Chlorophyllide a oxygenase; CC, Cellular component; CHIM, Mg-protoporphyrin IX methyltransferase; CPOX, Coproporphyrinogen III oxidative decarboxylase; CS, Chlorophyll synthase; DEGs, Differentially expressed genes; DVR, Divinyl reductase; GO, Gene Ontology; Glu-tRNAs, Glutamyl-tRNA reductase; GSA, Glutamate 1-semialdehyde aminomutase; Hmb, Hydroxymethylbilane; KEGG, Kyoto Encyclopedia of Genes and Genome; MgCH, Mg chelatase; MF, Molecular function; Mg-ProtoIX Cyclase, Mg-protoporphyrinogen IX monomethylester cyclase; NCBI, National Center for Biotechnology Information; PBGD, Porphobilinogen deaminase; POR, Protochlorophyllide oxidoreductase; PPO, Protoporphyrinogen oxidase; Proto IX,

Protoporphyrin IX; RNA-Seq, RNA sequencing; RT-qPCR, Real-time quantitative PCR; Urogen III, Uroporphyrinogen III; UROD, Uroporphyrinogen III decarboxylase; UROS, Uroporphyrinogen III synthase

Supplementary materials

Supplementary materials related to this article can be found, in the online version, at doi:.

Declarations

Acknowledgments

The authors would like to thank Wuhan Fraser Gene Information Co., Ltd. (Wuhan, China) for assisting with RNA-seq.

Author contributions

C.F and X.Z were the designers of this research scheme. H.W was the main experimental designer and data analyst. B. Z was the main sample gatherer and experimental operator. All authors read and approved the final manuscript.

Founding

The study received funding support from the Scientific and Technological Innovation Programs of Higher Education Institutions in Shanxi (Grant number: 82060779) and Luliang City to introduce high-level scientific and technological talents key research and development projects (Grant number:2023RC26)

Ethics approval and consent to participate

Not applicable.

Consent for publication

Not applicable.

Competing Interest

All authors declare that there are no competing interests in this research paper that affect publication.

Data availability

The obtained raw reads from RNAseq were deposited in the National Center for Biotechnology Information (NCBI) under submission number SUB14054825 and associated with Bioproject PRJNA1052366. These metabolome data can be accessed through the URL www.ebi.ac.uk/metabolights/MTBLS9474 using the unique identifier MTBLS9474.

References

1. Li Y, Xie L, Liu K, Li X, Xie F. Bioactive components and beneficial bioactivities of flowers, stems, leaves of *Lonicera japonica* Thunberg: a review. Biochem Syst Ecol. 2023;106:104570.

2. Beale SI. Green genes gleaned. Trends Plant Sci. 2005;10:309–312.

3. Li J, Yu X, Cai Z, Wu F, Luo J, Zheng L, Chu W. An overview of chlorophyll biosynthesis in higher plants. Mol Plant Breed. 2019;17:6013–6019.

4. Zeng ZQ, Lin TZ, Zhao JY, Zheng TH, Xu LF, Wang YH, Liu LL, Jiang L, Chen SH, Wan JM.

OsHemA gene, encoding glutamyl-tRNA reductase (GluTR) is essential for chlorophyll biosynthesis in rice (*Oryza sativa*). J Integr Agric. 2020;19:612–623.

5. Xu D, Sun D, Diao Y, Liu M, Gao J, Wu B, Yuan X, Lu P, Zhang Z, Zhang J, Guo G. Fast mapping of a chlorophyll *b* synthesis-deficiency gene in barley (*Hordeum vulgare* L.) via bulked-segregant analysis with reduced-representation sequencing. Crop J. 2019;7:58–64.

6. Papenbrock J, Gräfe S, Kruse E, Hänel F, Grimm B., 1997. Mg-chelatase of tobacco: identification of a *Chl D* cDNA sequence encoding a third subunit, analysis of the interaction of the three subunits with the yeast two-hybrid system, and reconstitution of the enzyme activity by co-expression of recombinant CHL D, CHL H and CHL I. Plant J. 1997;12:981–990.

7. Sawers RJH, Viney J, Farmer PR, Bussey RR, Olsefski G, Anufrikova K, Hunter CN, Brutnell TP, 2006. The maize *Oil Yellow1 (Oy1)* gene encodes the I subunit of magnesium chelatase. Plant Mol Biol. 2006;60:95–106.

8. Gong Z, Xiong L, Shi H, Yang S, Herrera-Estrella LR., Xu G, Chao DY, Li J, Wang PY, Qin F, Li J, Ding Y, Shi Y, Wang Y, Yang Y, Guo Y, Zhu JK. Plant abiotic stress response and nutrient use efficiency. Sci China Life Sci. 2020;63:635–674.

9. Salami M, Saadat S. Effects of drought stress on chlorophyll content changes of maize cultivars under field conditions. Int J Farming Allied Sci. 2013;2:167–169.

10. Cornic G. Drought stress inhibits photosynthesis by decreasing stomatal aperture–not by affecting ATP synthesis. Trends Plant Sci. 2000;5:187–188.

11. Ghotbi-Ravandi AA, Shahbazi M, Shariati M, Mulo P. Effects of mild and severe drought stress on photosynthetic efficiency in tolerant and susceptible barley (*Hordeum vulgare* L.) genotypes. J Agron Crop Sci. 2015;200:403–415.

12. Paknejad F, Nasri M, Moghadam HRT, Zahedi H, Alahmadi MJ. Effects of drought stress on chlorophyll fluorescence parameters, chlorophyll content and grain yield of wheat cultivars. J Biol Sci. 2007;7:841–847.

13. Ma XM, Wu CF. Effects of drought stress on physiological indicators and quality of *Lonicera japonica*. Guizhou Agric Sci. 2017;45:37–39.

14. Ma XM, Wu CF. Effects of drought stress on chlorophyll content and fluorescence characteristics in leaves of *Lonicera japonica*. Jiangsu Agric Sci. 2018;46:133–136.

15. Zhao J, Lang Y, Zhang S, Zhao Q, Zhang C, Xia J. Photosynthetic characteristics and chlorophyll a fluorescence transient in *Lonicera japonica* under drought stress. Acta Physiol Plant 2019;41:124.

16. Li J, Ju L, Zhang L, Sun P, Li M, Li J, Liu Y. Research progress on *Lonicera japottica* Thunb. Affected by environmental stress. Agric Biotechnol. 2022;11:12–18.

17. Yang B, Zhong Z, Wang T, Ou Y, Tian J, Komatsu S, Zhang L. Integrative omics of *Lonicera japonica* Thunb. Flower development unravels molecular changes regulating secondary metabolites. J Proteom. 2019;208:103470.

18. Xue Q, Fan H, Yao F, Cao X, Liu M, Sun J, Liu Y. Transcriptomics and targeted metabolomics profilings for elucidation of pigmentation in *Lonicera japonica* flowers at

842 different developmental stages. Ind Crops Prod. 2020;145:111981.
843 19. Xia Y, Chen W, Xiang W, Wang D, Xue B, Liu X, Xing L, Wu D, Wang S, Guo Q, Liang G.
844 Integrated metabolic profiling and transcriptome analysis of pigment accumulation in
845 *Lonicera japonica* flower petals during colour-transition. BMC Plant Biol. 2021;21:98.
846 20. Wang ZT, Zhou QY, Tian J. Identification and analysis on chlorophyll systhesis gene families
847 in *Allium sativum* under drought. J. Plant Res Environ. 2022;31:54–64.
848 21. Chen Y, Chen Y, Shi C, Huang Z, Zhang Y, Li S, Li Y, Ye J, Yu C, Li Z, Zhang X, Wang J,
849 Yang H, Fang L, Chen Q. SOAPnuke: a MapReduce acceleration-supported software for
850 integrated quality control and preprocessing of high-throughput sequencing data.
851 GigaScience. 2018;7:gix120.
852 22. Pu X, Li Z, Tian Y, Gao R, Hao L, Hu Y, He C, Sun W, Xu M, Peters RJ, Van de Peer Y, Xu
853 Z, Song J. The honeysuckle genome provides insight into the molecular mechanism of
854 carotenoid metabolism underlying dynamic flower coloration. New Phytol.
855 2020;227:930–943.
856 23 Kim D, Langmead B, Salzberg SL. HISAT: a fast spliced aligner with low memory
857 requirements. Nat. Methods. 2015;12:357–360.
858 24..Li B, Dewey CN. RSEM: accurate transcript quantification from RNA-Seq data with or
859 without a reference genome. BMC Bioinform. 2011;12:323.
860 25. Langmead B. Aligning short sequencing reads with bowtie. Curr Protoc Bioinform. 2010.
861 doi:10.1002/0471250953.bi1107s32.

862 26. Trapnell C, Williams BA, Pertea G, Mortazavi A, Kwan G, Van Baren MJ, Salzberg SL,
863 Wold BJ, Pachter L.Transcript assembly and quantification by RNA-Seq reveals
864 unannotated transcripts and isoform switching during cell differentiation. Nat Biotechnol.
865 2010;28,511–515.
866 27. Love MI, Huber W, Anders S. Moderated estimation of fold change and dispersion for
867 RNA-seq data with DESeq2. Genome Biol. 2014;15:550.
868 28. Young MD, Wakefield MJ, Smyth GK, Oshlack A. Gene ontology analysis for RNA-seq:
869 accounting for selection bias. Genome Biol. 2010;11:R14.
870 29. Mao X, Cai T, Olyarchuk JG, Wei L. Automated genome annotation and pathway
871 identification using the KEGG Orthology (KO) as a controlled vocabulary.
872 Bioinformatics. 2005;21:3787–3793.
873 30. Zhang M, Li M, Fu H, Wang K, Tian X, Qiu R, Liu J, Gao S, Zhong Z, Yang B, Zhang L.
874 Transcriptomic analysis unravels the molecular response of *Lonicera japonica* leaves to
875 chilling stress. Front Plant Sci. 2022;13:1092857.
876 31. Livak KJ, Schmittgen TD. Analysis of relative gene expression data using real-time
877 quantitative PCR and the $2^{-\Delta\Delta CT}$ method. Methods. 2001;25:402–408.
878 32. Hetherington AM, Woodward FI. The role of stomata in sensing and driving environmental
879 change. Nature. 2003;424:901–908.
880 33. McDonald PG, Fonseca CR, McC OJ, Westoby M. Leaf-size divergence along rainfall and
881 soil-nutrient gradients: is the method of size reduction common among clades? Funct.

Ecol. 2003;17:50–57.

34. Balota M, Payne WA, Evett SR, Peters TR. Morphological and physiological traits associated with canopy temperature depression in three closely related wheat lines. Crop Sci. 2008;48:1897–1910.

35. Zhang Y, Leng H, Cao H. Study on the influence of drought stress on botany. Heilongjiang Sci. 2022;13:22–24.

36. Rambabu B, Padma V, Thatikunta R, Sunil N. Effect of drought stress on chlorophyll content and anti-oxidant enzymes of green gram genotypes (*Vigna radiata* L.). Nat. Environ. Pollut. Technol. 2016;15:1205–1208.

37. Tanaka Y, Ohmiya A. Seeing is believing: engineering anthocyanin and carotenoid biosynthetic pathways. Curr Opin Biotechnol. 2008;19:190–197.

38. Tanaka Y. Flower colour and cytochromes P450. Phytochem Rev. 2006;5:283–291.

39. Dalal VK, Tripathy BC. Modulation of chlorophyll biosynthesis by water stress in rice seedlings during chloroplast biogenesis. Plant Cell Environ. 2012;35:1685–1703.

40. Ma Y, Zhang JH, Gao YN, Xu LX. Effect of ethephon on chlorophyll metabolism genes expression of Kentucky bluegrass under drought stres. Chin J Grassl. 2022; 44:1–10.

41. Quan R, Hu S, Zhang Z, Zhang H, Zhang Z, Huang R, 2010. Overexpression of an ERF transcription factor *TSRF1* improves rice drought tolerance. Plant Biotechnol J. 2010;8:476–488.

42. Fujino E, Fujino T, Karita S, Kimura T, Sakka K, Ohmiya K, 1999. Purification and

characterization of the *Clostridium josui* porphobilinogen deaminase encoded by the *hemC* gene from a recombinant *Escherichia coli*. J Biosci Bioeng. 1999;87:535–537.

43. Jensen PE, Gibson LCD, Henningsen KW, Hunter CN. Expression of the *chlI*, *chlD*, and *chlH* genes from the Cyanobacterium *Synechocystis* PCC6803 in *Escherichia coli* and demonstration that the three cognate proteins are required for magnesium-protoporphyrin chelatase activity. J Biol Chem. 1996;271:16662–16667.

44. Walker JC, Willows DR. Mechanism and regulation of Mg-chelatase. Biochem J. 1997; 327: 321–333.

45. Ipekoğlu EM, Göçmen K, Öz MT, Gürgan M, Yücel M. Cloning and heterologous expression of chlorophyll a synthase in *Rhodobacter sphaeroides*. J Basic Microbiol. 2017;57:238–244.

46. Nakagawara E, Sakuraba Y, Yamasato A, Tanaka R., Tanaka A. Clp protease controls chlorophyll *b* synthesis by regulating the level of chlorophyllide *a* oxygenase. Plant J. 2007;49:800–809.

47. Wang Y, Li XY, Li CX, He Y, Hou XY, Ma XR. The regulation of adaptation to cold and drought stresses in *Poa crymophila Keng* revealed by integrative transcriptomics and metabolomics analysis. Front Plant Sci. 2021;12:631117.

Supplementary Files

This is a list of supplementary files associated with this preprint. Click to download.

- Supplementarymaterials.zip